

# ZIKV induction of tristetraprolin in endothelial and Sertoli cells post-transcriptionally inhibits IFN $\beta$ / $\lambda$ expression and promotes ZIKV persistence

William R. Schutt,<sup>1,2</sup> Jonas N. Conde,<sup>1,2,3</sup> Megan C. Mladinich,<sup>1,2,3</sup> Grace E. Himmler,<sup>2,3</sup> Erich R. Mackow<sup>1,2</sup>

**AUTHOR AFFILIATIONS** See affiliation list on p. 15.

**ABSTRACT** Zika virus (ZIKV) is a mosquito-borne *Flavivirus* that persistently infects patients; enters protected brain, placental, and testicular compartments; is sexually transmitted; and causes fetal microcephaly *in utero*. ZIKV persistently infects human brain microvascular endothelial cells (hBMECs) that form the blood-brain barrier and Sertoli cells that form testicular barriers, establishing reservoirs that enable viral dissemination. ZIKV persistence requires inhibiting interferon (IFN) responses that direct viral clearance. We found that ZIKV induces IFN $\beta$  and IFN $\lambda$  in hBMECs but post-transcriptionally inhibits IFN $\beta$ /IFN $\lambda$  expression. IFN $\beta$ /IFN $\lambda$  mRNAs contain AU-rich elements (AREs) in their 3' untranslated regions which regulate protein expression through interactions with ARE-binding proteins (ARE-BPs). We found that ZIKV infection of primary hBMECs induces the expression of the ARE-BP tristetraprolin (TTP) and that TTP is a novel regulator of endothelial IFN secretion. In hBMECs, TTP knockout (KO) increased IFN $\beta$ /IFN $\lambda$  mRNA abundance and IFN $\beta$ /IFN $\lambda$  secretion in response to ZIKV infection and inhibited viral persistence. In contrast, TTP expression dramatically reduced IFN $\beta$ /IFN $\lambda$  secretion in hBMECs. IFN $\beta$ /IFN $\lambda$  mRNA stability was not significantly altered by TTP and is consistent with TTP inhibition of IFN $\beta$ /IFN $\lambda$  translation. TTP is similarly induced by ZIKV infection of Sertoli cells, and like hBMECs, TTP expression or KO inhibited or enhanced IFN $\beta$ /IFN $\lambda$  mRNA levels, respectively. These findings reveal a mechanism for ZIKV-induced TTP to promote viral persistence in hBMECs and Sertoli cells by post-transcriptionally regulating IFN $\beta$ /IFN $\lambda$  secretion. Our results demonstrate a novel role for virally induced TTP in regulating IFN secretion in barrier cells that normally restrict viral persistence and spread to protected compartments.

**IMPORTANCE** Our findings define a novel role for ZIKV-induced TTP expression in regulating IFN $\beta$ /IFN $\lambda$  production in primary hBMECs and Sertoli cells. These cells comprise key physiological barriers subverted by ZIKV to access brain and testicular compartments and serve as reservoirs for persistent replication and dissemination. We demonstrate for the first time that the ARE-binding protein TTP is virally induced and post-transcriptionally regulates IFN $\beta$ /IFN $\lambda$  secretion. In ZIKV-infected hBMEC and Sertoli cells, TTP knockout increased IFN $\beta$ /IFN $\lambda$  secretion, while TTP expression blocked IFN $\beta$ /IFN $\lambda$  secretion. The TTP-directed blockade of IFN secretion permits ZIKV spread and persistence in hBMECs and Sertoli cells and may similarly augment ZIKV spread across IFN $\lambda$ -protected placental barriers. Our work highlights the importance of post-transcriptional ZIKV regulation of IFN expression and secretion in cells that regulate viral access to protected compartments and defines a novel mechanism of ZIKV-regulated IFN responses which may facilitate neurovirulence and sexual transmission.

**KEYWORDS** Zika virus, tristetraprolin, endothelial cells, Sertoli cells, interferon regulation, persistence, post-transcriptional, secretion

**Editor** John T. Patton, Indiana University  
Bloomington, Bloomington, Indiana, USA

Address correspondence to Erich R. Mackow,  
Erich.Mackow@StonyBrook.edu.

The authors declare no conflict of interest.

See the funding table on p. 16.

**Received** 14 July 2023

**Accepted** 20 July 2023

**Published** 14 September 2023

Copyright © 2023 Schutt et al. This is an open-access  
article distributed under the terms of the [Creative  
Commons Attribution 4.0 International license](https://creativecommons.org/licenses/by/4.0/).

Zika virus (ZIKV) is a mosquito-borne neurovirulent *Flavivirus* that uniquely spreads sexually, persists for months in humans, and causes encephalitis and fetal microcephaly *in utero* (1–5). In adults, ZIKV is found persistently in saliva, urine, cerebrospinal fluid, and semen causing encephalitis, Guillian-Barre syndrome, and permitting sexual transmission (5–7). During pregnancy, ZIKV spreads across the placenta and establishes persistence in Hofbauer cells, fetal macrophages that serve as reservoirs for ZIKV fetal dissemination in infected humans and remain infected regardless of the gestational term at which initial infection occurred (8, 9). Subsequent viral spread and infection of the developing brain result in damage to fetal neurons, neural progenitors, and astrocytes that limit brain development and can result in characteristic fetal microcephaly (10, 11). Accordingly, ZIKV infects and crosses endothelial cell (EC), placental, and testicular barriers that normally restrict viral access to the central nervous system (CNS), fetal tissues, and semen (1, 7, 12–14). The blood-brain barrier (BBB) is a neurovascular complex formed by brain microvascular endothelial cells (BMECs), pericytes, and astrocytes that separate the brain from circulating blood constituents and pathogens. Our lab established that ZIKV persistently and non-lytically infects human brain microvascular endothelial cells (hBMECs), releasing progeny virus both apically and basolaterally without permeabilizing model BBBs (15–17). Additional studies have shown that Sertoli cells that form testicular barriers are persistently infected by ZIKV (18, 19). These findings suggest roles for hBMECs and Sertoli cells as ZIKV reservoirs that facilitate neuroinvasion and sexual transmission.

ECs are a unique cell type with distinct receptors, signaling pathways, and interferon (IFN)-directed responses that differentiate them from immune and epithelial cells and tailor their response to viral infection (20, 21). The endothelium is a target for many tick- and mosquito-borne flaviviruses that cause vascular or neurotropic diseases, including dengue virus (DENV), West Nile virus, and Powassan virus (22–24). ECs produce type I IFN $\beta$  and type III IFN $\lambda$  in response to viral infections and respond to IFN $\alpha$ /IFN $\beta$  through cognate type I IFN receptors (IFNARs). ECs lack IFN $\lambda$  receptors (IFN $\lambda$ Rs), and the addition of IFN $\lambda$  to cells fails to inhibit ZIKV infection or induce interferon-stimulated genes (ISGs). Prior treatment of cells with IFN $\alpha$ /IFN $\beta$  inhibits ZIKV and other *Flavivirus* infections, and DENV infection of human ECs induces IFN $\alpha$ /IFN $\beta$  secretion that inhibits DENV spread and ultimately leads to viral clearance (15, 24–26). In contrast, ZIKV persistently infects hBMECs without IFN $\beta$  secretion, spreading in monolayers for >9 days and following cellular passage (15, 17). Similar ZIKV persistence has been reported in Sertoli cells, an epithelial cell type that comprises the blood-testes barrier and is hypothesized to facilitate viral entry into the testes and contribute to long-term viral shedding and sexual transmission (18, 19, 27). How ZIKV persists within brain and testicular barrier cells is not fully understood; however, the ability of ZIKV to restrict IFN responses that prevent viral clearance is likely central to ZIKV's novel persistence, spread, and neurovirulence.

ZIKV has multiple mechanisms of inhibiting IFN responses both upstream and downstream of IFN induction and secretion (28). To impair viral RNA recognition, ZIKV inhibits the activation of retinoic acid-inducible gene I (RIG-I) and melanoma differentiation-associated protein 5 (MDA-5) via expression of several non-structural proteins and genomic sfRNA (29–34). ZIKV also inhibits IFN signaling directed by IFN receptor activation by inhibiting JAK-STAT2 signaling responses (25, 28, 35, 36). Despite suppression of the IFN induction and IFN signaling pathways, IFN $\beta$  and IFN $\lambda$  are induced by ZIKV infection of a variety of cell types including hBMECs and Sertoli cells (15, 37, 38). Although IFN was induced in ZIKV-infected hBMECs, we found that the expression and secretion of IFN $\beta$ /IFN $\lambda$  in cell supernatants were repressed below the limit of detection and failed to inhibit viral infection or spread (15). Secretory pathways were not globally altered by ZIKV as CCL5, a highly induced, pro-survival chemokine, was highly secreted into ZIKV-infected hBMEC supernatants. While most studies evaluate IFN transcripts as surrogates for IFN expression, a discrepancy between IFN $\beta$ /IFN $\lambda$  induction and secretion has also been reported following ZIKV infection of dendritic cells, peripheral blood mononuclear cells, fetal neural progenitor cells, and placental macrophages (9, 37, 39,

40). A mechanism for post-transcriptional regulation of IFN has not been proposed, and the absence of IFN secretion was hypothesized to result from inhibited IFN translation (37).

IFN $\beta$ /IFN $\lambda$  belong to a family of tightly regulated inflammatory cytokines, present at low endogenous levels, that undergo post-transcriptional regulation to rapidly repress secretion (41). Transcript regulation is reportedly mediated by the presence of AU-rich elements (AREs) found in 3' untranslated regions (UTRs) of cytokine mRNAs. ARE recognition sequences drive interactions with ARE-binding proteins (ARE-BPs) that positively or negatively regulate mRNA translation and stability (41–48). How AREs and ARE-BPs influence IFN $\beta$ /IFN $\lambda$  expression during ZIKV infection has not been investigated.

Studies involving the ARE-BP tristetraprolin (TTP) have largely focused on its role in lipopolysaccharide (LPS)-treated myeloid cells, with little understanding of its role in type I/type III IFN regulation or following viral infection. In ECs, expression of the TTP has been shown to regulate the expression of inflammatory cytokines (49, 50). TTP post-transcriptionally inhibits the expression of ARE-containing mRNAs through two separate mechanisms that may function independently or simultaneously (51). TTP can promote the degradation of ARE-mRNAs through deadenylation via recruitment of the CCR4-NOT exonuclease complexes or DCP1/2 decapping enzymes and Xrn1 digestion (52–57). TTP is also capable of translational repression via recruitment of inhibitory translational complexes to mRNAs that interfere with cap binding to eIF4E and translation initiation complex assembly (51, 58–61). How AREs and ARE-BPs influence IFN $\beta$ /IFN $\lambda$  expression during ZIKV infection has not been studied.

Here we investigate ZIKV-directed post-transcriptional regulation of IFN expression and define roles for ARE-binding proteins in ZIKV persistence in hBMECs and Sertoli cells. In contrast to ARE-BPs AUF1, HuR, and KHSRP, we found that TTP is uniquely induced in ZIKV-infected hBMECs and that knockout (KO) or expression of TTP, respectively, increases or blocks IFN $\beta$ /IFN $\lambda$  secretion. Our findings identify TTP as a ZIKV-induced protein in hBMECs and Sertoli cells that regulates the expression of IFN $\beta$  and IFN $\lambda$  by inhibiting their translation. In addition, we found that ZIKV induces TTP in primary human Sertoli cells (hSerC) and that TTP expression or KO regulates IFN $\beta$ /IFN $\lambda$  secretion. These findings reveal a post-transcriptional mechanism of ZIKV-directed IFN regulation resulting from TTP induction following infection and permit ZIKV persistence in cells that normally restrict viral entry into protected compartments.

## RESULTS

### ZIKV inhibits IFN secretion from hBMECs

We previously reported that ZIKV persistently infects hBMECs, transiently inducing IFN $\beta$  and IFN $\beta$ /IFN $\lambda$  without IFN $\beta$ /IFN $\lambda$  secretion (15). Here we extend these findings and define roles for the ARE-BP TTP in ZIKV-directed post-transcriptional regulation of IFN $\beta$ /IFN $\lambda$  in hBMECs. We infected primary hBMECs with ZIKV (PRVABC59) and monitored viral spread and the induction and secretion of IFN $\beta$  and IFN $\lambda$ . ZIKV titers increased from 24 to 72 hpi, and monolayers remained persistently infected despite passaging ZIKV-infected cells 3 and 6 dpi (Fig. 1A). Following ZIKV infection of hBMECs, we found that both IFN $\beta$  and IFN $\lambda_1$  were transcriptionally induced 1–3 dpi (Fig. 1B and C), but we failed to detect IFN $\beta$  or IFN $\lambda$  secretion into cell supernatants by enzyme-linked immunosorbent assay (ELISA) (Fig. 1D and E). In contrast, hBMECs transfected with poly(I:C) for 24 h directed the secretion of both IFN $\beta$ /IFN $\lambda_1$  (Fig. 1D and E). Concurrently treating hBMECs with IFN $\alpha$  during ZIKV infection reduced the number of infected cells by 80%, while IFN $\lambda$ -treated hBMECs had no effect on ZIKV infection (Fig. 1F). Consistent with this, ZIKV persistence and spread in hBMECs functionally demonstrate the absence of IFN $\beta$  secretion in ZIKV-infected hBMEC supernatants. Validating the presence of IFN $\alpha$ /IFN $\beta$ , but not IFN $\lambda$ , receptors on hBMECs, cellular ISGs (ISG15 and MXA) were transcriptionally induced by IFN $\alpha$  but not by IFN $\lambda$  addition to hBMECs (Fig. 1G). In contrast, treatment with both IFN $\alpha$  and IFN $\lambda$  induce ISGs in A549 cells (Fig. S1), demonstrating that hBMECs only express type I IFNARs and selectively respond to IFN $\alpha$ /IFN $\beta$ . Our findings indicate that

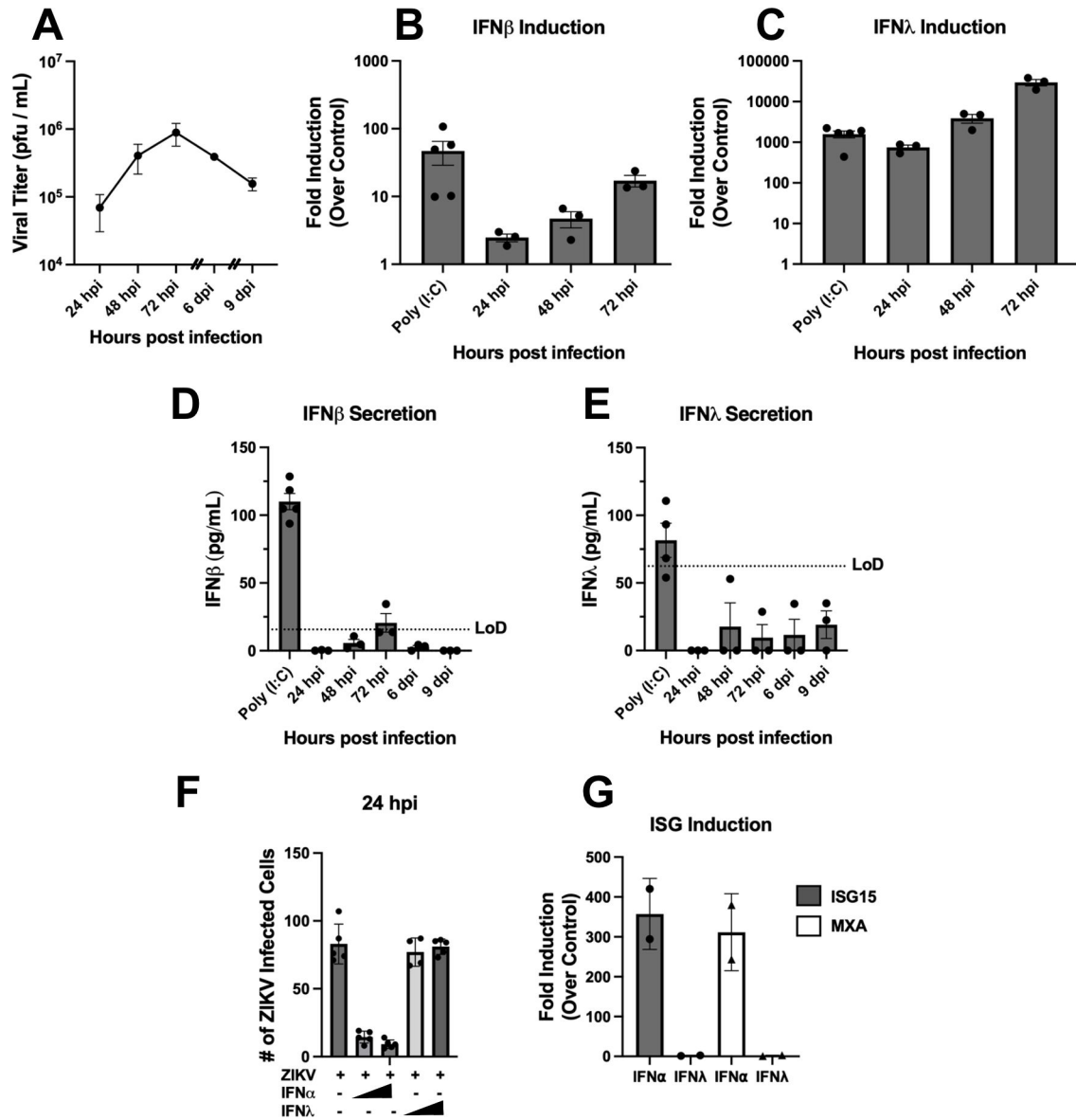


**FIG 1** ZIKV Inhibits IFN secretion in in hBMECs. (A) Primary hBMECs were ZIKV infected (multiplicity of infection [MOI] = 0.05) and supernatants collected at the indicated times. Hash marks indicate when infected hBMECs were trypsinized and passaged (3 and 6 dpi). Viral titers were determined by focus forming units (FFU) assay on Vero E6 cells. (B through E) RNA and supernatants from ZIKV-infected hBMECs (MOI 0.05) were collected. The induction of IFN $\beta$  (B) and IFN $\lambda$  (C) relative to uninfected control hBMECs was quantified via qRT-PCR and secreted IFN $\beta$  (D) and IFN $\lambda$  (E) determined by ELISA. (F and G) Wild-type (WT) hBMECs were ZIKV infected (MOI 0.5) with or without IFN $\alpha$  (1,000 or 2,000 U/mL) or IFN $\lambda_1$  (10 or 50 ng/mL) addition. The number of ZIKV antigen-positive hBMECs was quantified for 24 hpi using anti-DENV4 hyperimmune mouse ascitic fluid (F) and assessed for ISG induction relative to untreated controls ( $n = 2$ ) (G). Data are represented as the mean  $\pm$  standard error of the mean (SEM). Experiments were performed at least three times unless otherwise noted.

ZIKV infection of hBMECs post-transcriptionally inhibits IFN $\beta$ /IFN $\lambda$  expression to facilitate ZIKV persistence and spread.

### The ARE-BP TTP is induced by ZIKV infection and localized to the cytoplasm

It is widely reported that ZIKV infection transcriptionally induces IFN $\beta$ /IFN $\lambda$ . To explain the discrepancy between IFN mRNA levels and a lack of protein secretion, we hypothesized that ZIKV regulates IFN expression and secretion at a post-transcriptional level. We first performed a miRNA screen of ZIKV-infected hBMECs at 24 hpi but failed to detect significant upregulation of any canonical IFN $\beta$ /IFN $\lambda$  targeting miRNAs (data not shown).

Based on the potential roles of AREs in cytokine 3' UTRs regulating mRNA expression, we evaluated the expression of ARE-BPs in response to ZIKV infection of hBMECs. IFN $\beta$  and IFN $\lambda$  contain 3' UTR ARE domains that may regulate IFN expression in a cell type specific manner, and thus these experiments were performed in biologically relevant hBMECs in which post-transcriptional regulation has been observed (41, 42, 48). We evaluated expression levels of ARE-BPs HuR, KHSRP, AUF1, and TTP in ZIKV-infected hBMECs 1–3 dpi. We found that AUF1, HuR, and KHSRP were expressed constitutively in mock and ZIKV-infected hBMECs, with no change in expression following ZIKV infection (Fig. 2A). In contrast, TTP is expressed at extremely low constitutive levels in hBMECs and highly induced by ZIKV 1–3 dpi compared to mock-infected cells.

Regulation of mRNAs by ARE-BPs is linked to protein activation that directs localization from the nucleus to the cytoplasm (62–65). We evaluated ARE-BP localization in ZIKV versus mock-infected cells for 24 hpi and observed no change in the nuclear or cytoplasmic localization of AUF1 or KHSRP in mock- or ZIKV-infected hBMECs (Fig. 2B). The absence of TTP in mock-infected cells prevents analysis of a change in TTP localization, but the exclusive localization of TTP in the cytoplasm of ZIKV-infected hBMECs indicates the unique induction of activated TTP in ZIKV-infected hBMECs (Fig. 2B).

### ZIKV induction of TTP is independent of IRF3 and IFN

TTP induction has primarily been studied in myeloid cells in response to inflammatory LPS and tumor necrosis factor alpha (TNF- $\alpha$ ) stimuli, while the role of IFNs is unclear (62, 66). As IFN $\beta$ /IFN $\lambda$  secretion is restricted in ZIKV-infected hBMECs, we compared TTP induction in response to ZIKV infection or stimulation with IFN $\alpha$ /IFN $\lambda$ . hBMECs were ZIKV infected, treated with 1,000 U/mL of IFN $\alpha$  or 50 ng/mL of IFN $\lambda$  for 24 h prior to analysis of TTP induction by qRT-PCR (Fig. 3A). We found that ZIKV virus infection, but not IFN $\alpha$ /IFN $\lambda$  treatment, induced TTP in hBMECs. These findings are consistent with a previous study indicating that knockdown of RIG-I partially reduced TTP induction in response to RNA transfection (67). To determine if TTP induction is mediated by IRF3 activation following ZIKV infection, we transduced hBMECs to express a dominant negative IRF3 (IRF3 $\Delta$ 60)

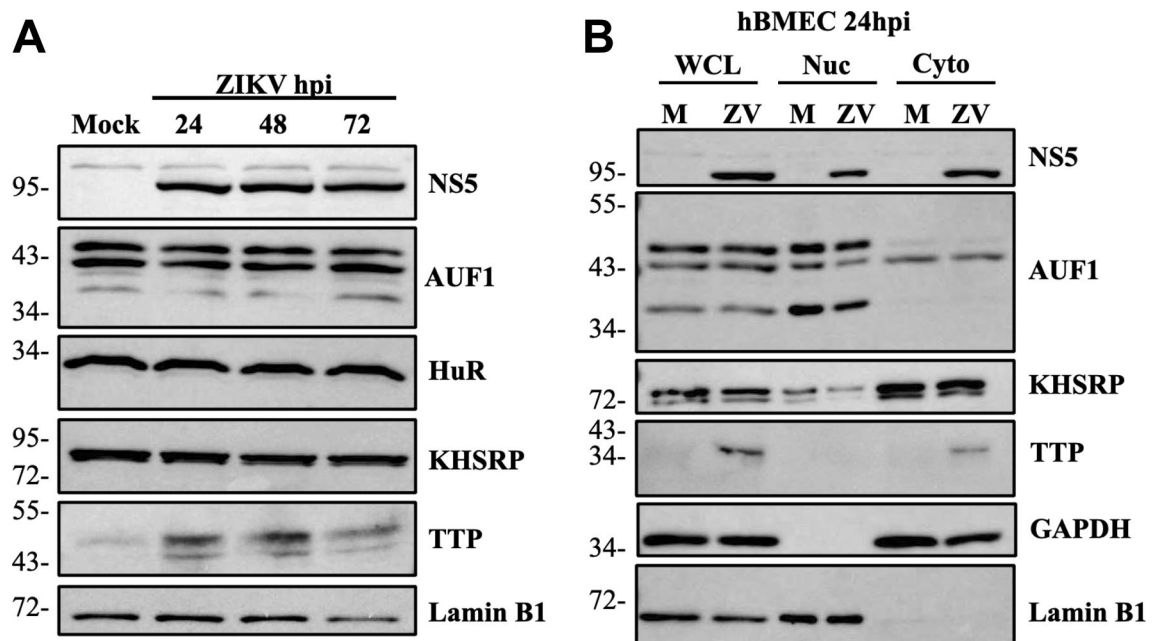


**FIG 2** ZIKV induces TTP in the cytoplasm of hBMEC infection. (A) Primary hBMECs were ZIKV infected (MOI 1.0), and lysates were evaluated for the expression of ARE-BPs assessed by Western blot. (B) Mock and ZIKV-infected hBMECs (MOI 1.0) were lysed, and whole cell lysate was collected prior to centrifugation and splitting of cytoplasmic (Cyto) and nuclear (Nuc) fractions. Lysates were Western blotted for cytoplasmic glyceraldehyde 3-phosphate dehydrogenase (GAPDH) and nuclear lamin B1 protein markers to confirm localization and equal loading. Western blots are representative of multiple independent experiments.

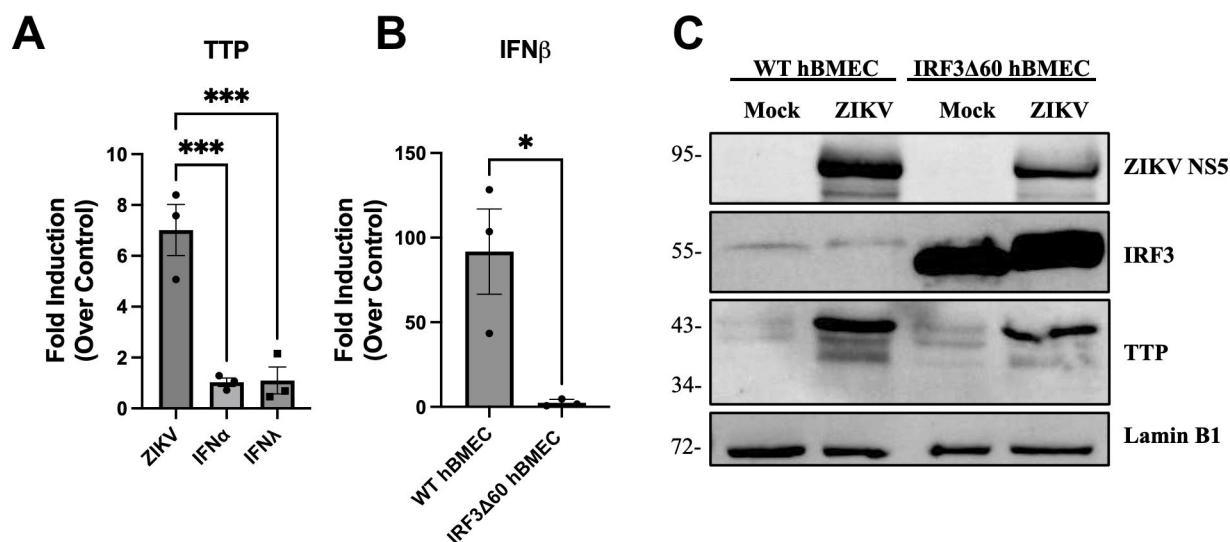


**FIG 3** ZIKV induction of TTP is independent of IRF3 and IFN. (A) Primary hBMECs were ZIKV infected (MOI 10) and treated with exogenous IFN $\alpha$  (1,000 U/mL) or IFN $\lambda$  (50 ng/mL) for 24 hpi prior to analysis of TTP transcripts by qRT-PCR relative to untreated control hBMECs. Statistical significance was determined by one-way analysis of variance (ANOVA). (B and C) Primary hBMEC and hBMECs expressing dominant negative IRF3 $\Delta$ 60 were ZIKV infected (MOI 10), and the transcriptional induction of IFN $\beta$  was determined by qRT-PCR relative to uninfected WT or IRF3 $\Delta$ 60-hBMECs (B) with significance defined by unpaired Student's *t* test. Expression of IRF3 and TTP were analyzed by Western blot (C). Data are represented as the mean  $\pm$  SEM; asterisks indicate statistical significance. \**P*  $\leq$  0.05, \*\*\**P*  $\leq$  0.001. Experiments were performed three times.

that lacks the ability to induce IFN $\beta$  (68). In response to ZIKV infection, IFN $\beta$  was induced in WT hBMECs but not IRF3 $\Delta$ 60-hBMECs, and IRF3 $\Delta$ 60 expression dramatically reduced IRF3-directed ISG expression (Fig. 3B; Fig. S2). Protein analysis revealed that TTP expression was induced by ZIKV infection of both WT and IRF3 $\Delta$ 60 hBMECs (Fig. 3C). These findings demonstrate that ZIKV infection of endothelial cells transcriptionally induces TTP expression independently of IRF3 or IFN signaling responses.

### TTP expression inhibits IFN $\beta$ /IFN $\lambda$ expression

While TTP has been shown to inhibit the expression of some ARE-containing cytokines, regulation of IFNs remains understudied and has only been addressed in immune cells. To evaluate the effect of TTP on IFN $\beta$ /IFN $\lambda$  induction and secretion in hBMECs, we generated TTP CRISPR-Cas9 KO and doxycycline-induced TTP overexpressing hBMECs (Fig. S3). Following poly(I:C) transfection, TTP KO hBMECs exhibited higher induction of IFN $\beta$ /IFN $\lambda$  that was dramatically reduced by TTP overexpression (Fig. 4A and B). The enhanced IFN mRNA abundance corresponded with a significant increase in IFN $\beta$ /IFN $\lambda$  secretion by TTP KO cells 24 h post-transfection (Fig. 4C and D). These findings demonstrate direct and novel IFN $\beta$ /IFN $\lambda$  regulation by TTP in endothelial cells and suggest a mechanism for virally induced TTP to modulate inflammatory responses of the endothelium.

### ZIKV persistence is suppressed in TTP KO and enhanced in TTP-expressing hBMECs

We determined if TTP KO or TTP expression in hBMECs affected ZIKV replication and persistence in hBMECs. In a synchronous ZIKV infection of WT, TTP KO, and TTP-expressing hBMECs, we found that titers rapidly reached maximal levels ( $1 \times 10^6$  /mL) 1–3 dpi with little difference between cell types (Fig. 5A). To assess roles for TTP in viral persistence, we passaged ZIKV-infected WT, TTP KO, and TTP-expressing cells at 3 and 6 dpi and monitored viral titers 6–9 dpi (Fig. 5B). We observed a significant reduction in persistently infected ZIKV titers in TTP KO hBMECs at 6 and 9 dpi versus hBMECs that express TTP (WT or TTP expressing). In support of TTP-regulated ZIKV persistence,

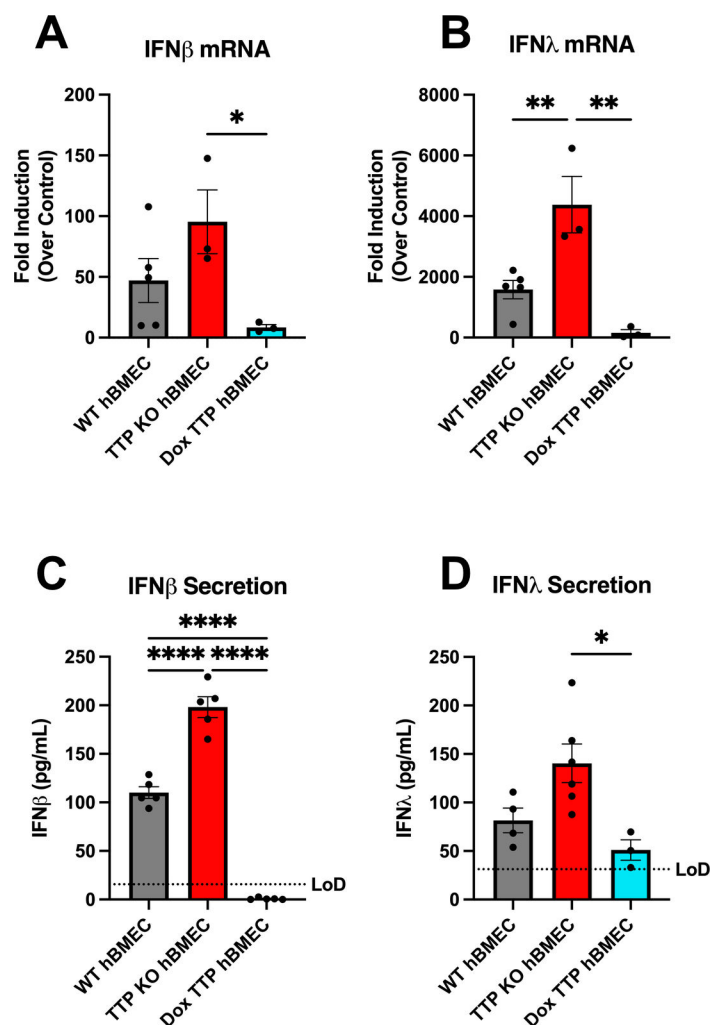


**FIG 4** TTP expression inhibits IFN $\beta$ /IFN $\lambda$  expression. Primary hBMECs, TTP-KO hBMECs, and TTP-expressing hBMECs were poly (I:C) transfected (0.5  $\mu$ g/mL) using FuGENE 6 for 24 h prior to the collection of RNA and supernatants. TTP was doxycycline (Dox) induced (200 ng/mL) throughout the course of the experiment. Transcriptional induction of IFN $\beta$  (A) and IFN $\lambda_1$  (B) was determined by qRT-PCR and normalized to untreated, uninfected WT, TTP KO, and Dox TTP controls. hBMEC supernatants were assayed for IFN $\beta$  (C) and IFN $\lambda$  (D) by ELISA. Data are presented as the mean  $\pm$  SEM; asterisks indicate statistical significance as determined by one-way ANOVA. \* $P \leq 0.05$ , \*\* $P \leq 0.001$ , \*\*\* $P \leq 0.0001$ . Experiments were performed at least three times.

staining of ZIKV-infected hBMECs 6–9 dpi revealed reduced ZIKV spread in TTP KO cells versus WT or TTP-expressing hBMECs (Fig. 5C). Collectively, these findings suggest that ZIKV-induced TTP expression suppresses IFN secretion and facilitates persistent viral spread.

We evaluated IFN $\beta$ /IFN $\lambda$  induction and secretion in WT, TTP KO, and TTP-expressing hBMECs following synchronous (MOI = 10) ZIKV infection. In TTP KO cells, IFN $\beta$ /IFN $\lambda_1$  was induced two- to fourfold over WT hBMECs 1–3 dpi (Fig. 6A and B). In contrast, TTP-expressing cells dramatically repressed IFN $\beta$ /IFN $\lambda$  induction 5–10 fold versus WT or TTP KOs (Fig. 6A and B). The secretion of IFN $\beta$  was notably enhanced in ZIKV-infected TTP KO hBMECs 1–3 dpi, with TTP-expressing hBMECs repressing IFN $\beta$  secretion to levels 5- to 30-fold less than WT or TTP KO cells (Fig. 6C through E). A similar trend of IFN $\lambda$  secretion 2–3 dpi in TTP KOs and reduced IFN $\lambda$  secretion in TTP-expressing cells was observed but diminished (Fig. 6F through H). These findings reveal a novel mechanism of ZIKV-directed post-transcriptional IFN regulation directed by the induction of the ARE-BP TTP and

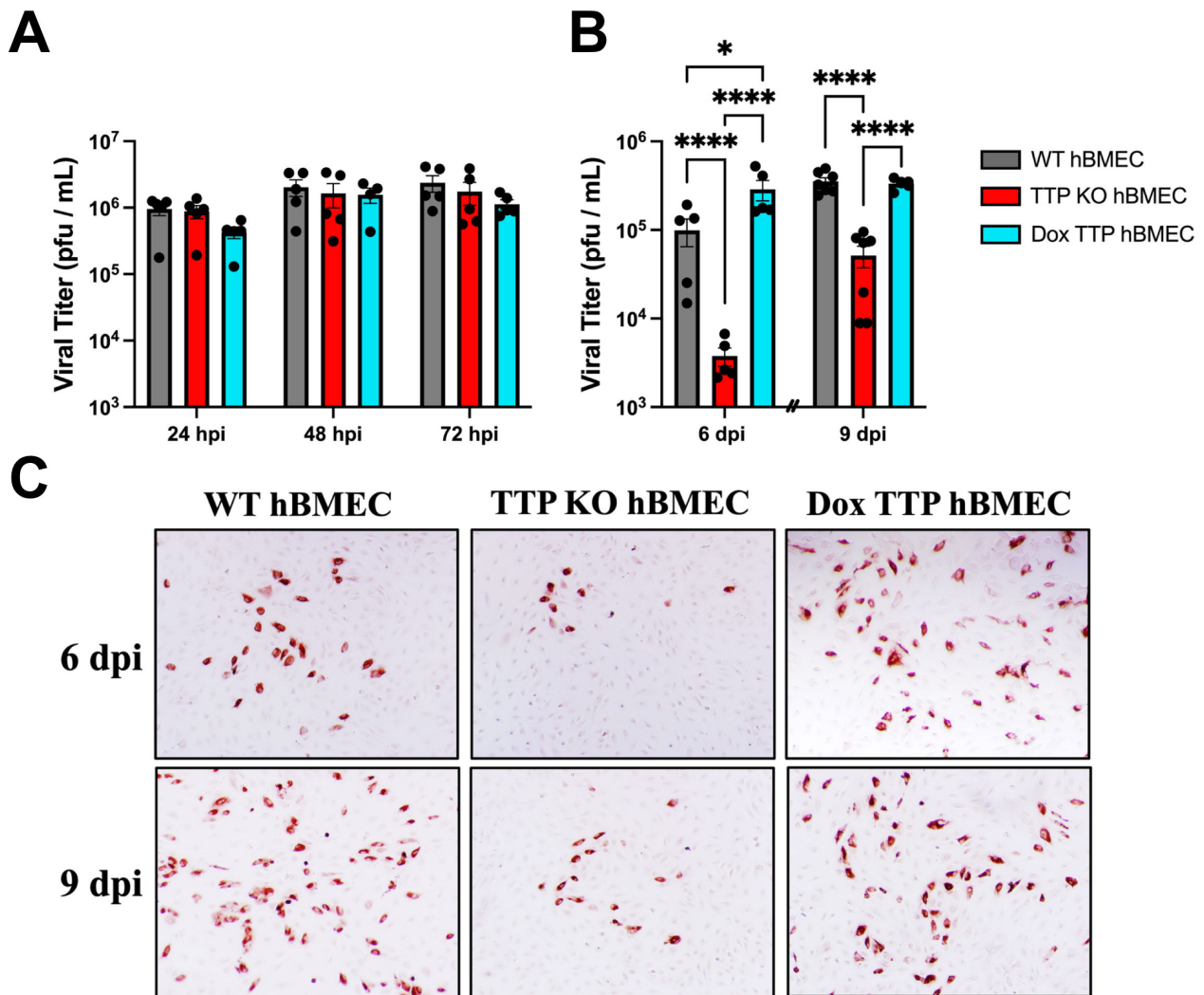


**FIG 5** ZIKV persistence is suppressed in TTP KOs and enhanced in TTP-expressing hBMECs. (A and B) Primary hBMECs, TTP-KO hBMECs, and TTP-expressing hBMECs were ZIKV infected (MOI = 1), and supernatants were collected and titered on Vero E6 cells at the indicated times. (B) Infected hBMECs were trypsinized and passaged at 3 and 6 dpi (hash marks and titers quantified 3 days after passage). Data are presented as the mean ± SEM; asterisks indicate statistical significance as determined by two-way ANOVA of log<sub>10</sub>-transformed titers. \**P* ≤ 0.05, \*\*\*\**P* ≤ 0.0001. Experiments were performed four times. (C) Infected hBMECs were fixed, and ZIKV-positive cells were stained with anti-DENV4 hyperimmune mouse ascitic fluid at 6 and 9 dpi.

demonstrates a novel role for ZIKV-induced TTP in regulating viral persistence and spread in endothelial cells.

### TTP KO does not alter IFN mRNA degradation

In immune cells, TTP has been shown to post-transcriptionally repress cytokine expression through TTP complexes that translationally repress protein expression from ARE containing mRNAs or reduce the stability of ARE-mRNA transcripts. To differentiate TTP mechanisms of action, we evaluated the rate of IFNβ/IFNλ mRNA degradation in WT and TTP KO cells and compared the effect of TTP to the canonical TTP destabilizing target interleukin-6 (IL-6). WT hBMECs and TTP KO hBMECs were ZIKV infected (MOI = 10) and treated with actinomycin D (ActD) at 20 hpi to block new RNA transcription and were assayed for changes in IFNβ/IFNλ and IL-6 mRNA abundance (2–4 h post-ActD addition) by qRT-PCR. In TTP KO hBMECs, there was a noted reduction in the rate of IL-6 mRNA degradation that reflects the role of TTP in reducing IL-6 mRNA stability in immune cells (Fig. 7C) (69). In contrast, in ZIKV-infected hBMECs, TTP KO did not significantly alter the



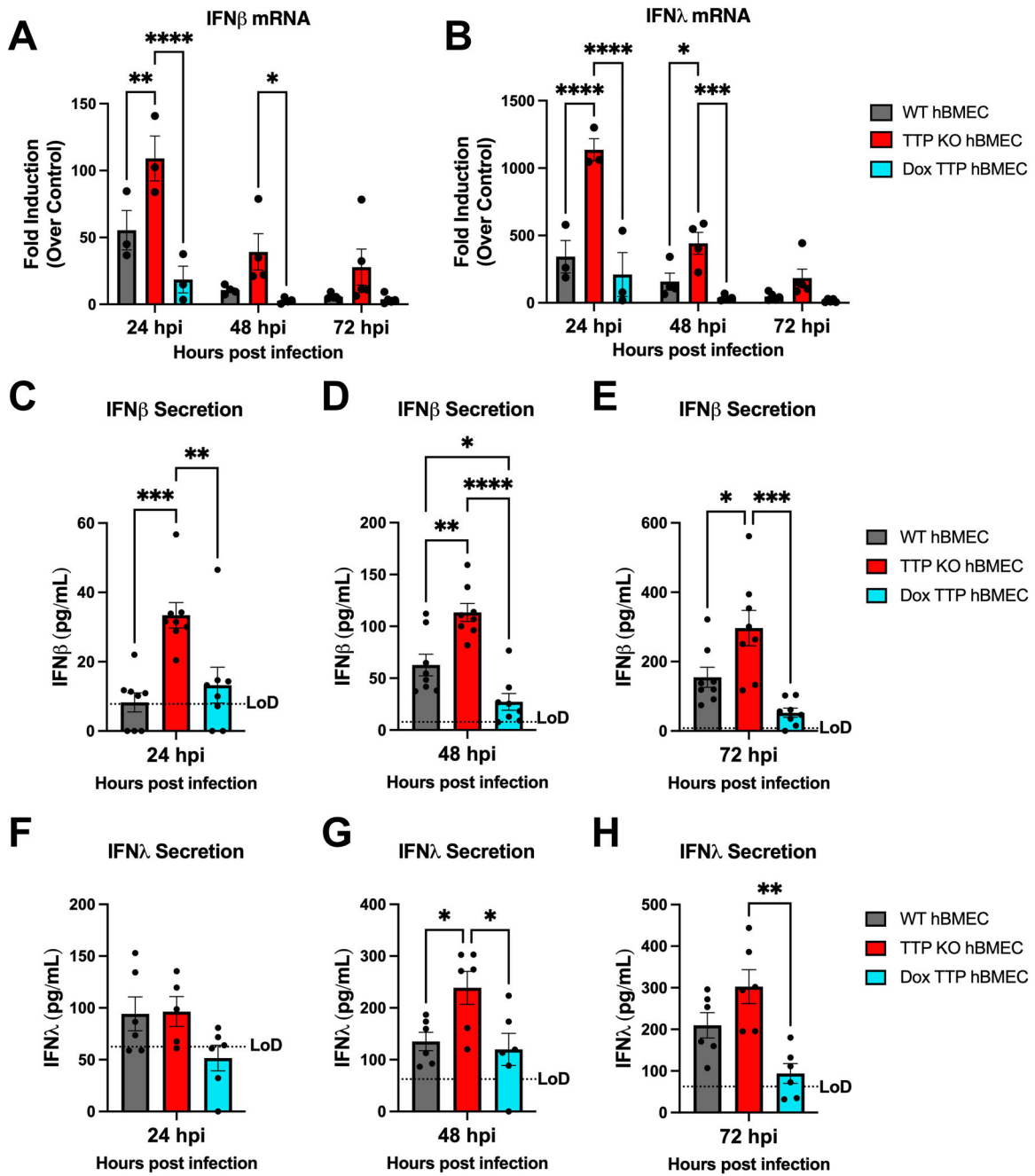


**FIG 6** IFN induction and secretion is enhanced in ZIKV-infected TTP KO hBMECs. Primary hBMECs, TTP-KO hBMECs, and TTP-expressing hBMECs were ZIKV infected (MOI = 10), and at the indicated times, IFN $\beta$  (A) and IFN $\lambda$  (B) mRNAs were quantified by qRT-PCR relative to uninfected WT, TTP KO, and Dox TTP controls, and secreted IFN $\beta$  (C through E) and IFN $\lambda$  (F through H) were assayed by ELISA (R&D Systems). Data are presented as the mean  $\pm$  SEM; asterisks indicate statistical significance as determined by two-way ANOVA. \* $P \leq 0.05$ ; \*\* $P \leq 0.002$ ; \*\*\* $P \leq 0.0002$ ; \*\*\*\* $P \leq 0.0001$ . Experiments were performed four times.

rate of IFN $\beta$  or IFN $\lambda$  mRNA degradation compared to WT hBMECs (Fig. 7A and B). These findings are consistent with TTP inhibiting IFN $\beta$ /IFN $\lambda$  secretion through the post-transcriptional inhibition of IFN $\beta$ /IFN $\lambda$  mRNA translation in hBMECs.

### TTP regulates IFN $\beta$ /IFN $\lambda$ expression in hSerCs

ZIKV persistently infects human Sertoli cells that protect testicular compartments, and viral persistence in this cellular niche is likely to enhance ZIKV sexual transmission (18, 19, 70). Sertoli cells produce both IFN $\beta$  and IFN $\lambda$  and are sensitive to exogenous type I IFN

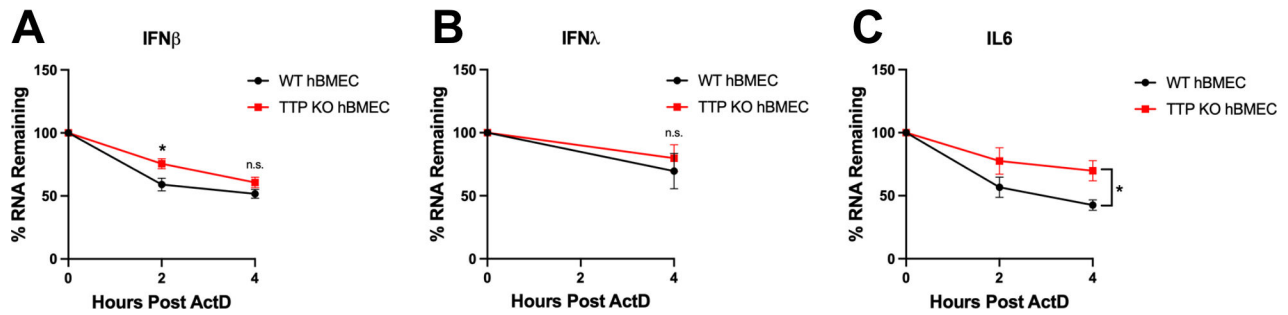


**FIG 7** TTP KO does not alter IFN mRNA stability. Primary hBMECs and TTP-KO hBMECs were ZIKV infected (MOI = 10) for 20 h prior to the addition of actinomycin D (5  $\mu$ g/mL). RNA was collected 0, 2, and 4 h post-ActD addition, and the levels of IFN $\beta$  (A), IFN $\lambda_1$  (B), and IL-6 (C) mRNAs were analyzed via qRT-PCR and normalized to  $\beta$ -actin relative to the 0-h time point. Data are represented as the mean  $\pm$  SEM; asterisks indicate statistical significance as determined by two-way ANOVA. \* $P \leq 0.05$ . Experiments were performed three times. n.s., not significant.

treatment (Fig. 8A). Like hBMECs, the addition of IFN $\lambda$  to Sertoli cells does not restrict ZIKV replication or induce ISGs (Fig. 8A through C, 1G and H). We initially determined if ZIKV infection directs ARE-BP responses that inhibit IFN $\beta$ /IFN $\lambda$  secretion in hSerCs. Primary hSerCs were synchronously infected with ZIKV, and the expression of ARE-BPs was monitored 1–2 dpi. Like hBMECs, hSerCs showed no alteration in HuR, KHSRP, or AUF1 expression following ZIKV infection (Fig. 8D). In contrast, TTP expression was dramatically increased in ZIKV-infected Sertoli cells 1–2 dpi (Fig. 8D). To evaluate the role of TTP in regulating IFN $\beta$ /IFN $\lambda$  mRNA levels in Sertoli cells, we generated TTP-KO and TTP-expressing hSerCs (Fig. S4). ZIKV-infected TTP KO hSerCs demonstrated a dramatic increase in IFN $\beta$ /IFN $\lambda$  mRNA levels compared to ZIKV-infected WT controls (Fig. 8E and F). Conversely, ZIKV infection of TTP-expressing hSerCs reduced IFN $\beta$ /IFN $\lambda$  mRNA levels by 60–85% when compared to WT or TTP-KO hSerCs (Fig. 8E and F). These findings demonstrate that ZIKV-induced TTP regulates IFN $\beta$ /IFN $\lambda$  expression in Sertoli cells, key testicular barrier cells that serve as reservoirs for ZIKV dissemination and contribute to sexual transmission. ZIKV-directed TTP induction and IFN regulation reveal a fundamental ZIKV persistence mechanism that may prevent viral clearance from crucial physiological barriers.

## DISCUSSION

ZIKV is distinguished from other flaviviruses by its ability to persist in patients for up to 6 months, cause fetal microcephaly *in utero*, and be sexually transmitted (1–4, 71). To accomplish this, ZIKV persistently infects endothelial, trophoblast, and Sertoli cells that serve as barriers to immune protected brain, testicular, and placental compartments (12, 72–75). ZIKV persistence provides a reservoir for ZIKV dissemination and spread across tissue restrictive barriers (15). We previously reported that ZIKV persistently infects blood-brain barrier endothelial cells, spreading basolaterally from polarized hBMECs, a mechanism consistent with CNS entry. ZIKV persistence in hBMECs requires the autocrine activation of pro-survival CCL5 responses and the inhibition of IFN $\beta$  secretion (17). hBMECs secrete type I (IFN $\beta$ ) and type III (IFN $\lambda$ ) IFNs; however, as hBMECs lack IFN $\lambda$ R and fail to respond to IFN $\lambda$ , ZIKV infection of hBMECs is only restricted by type I IFN pre-treatment. Despite transient induction of IFN $\beta$ /IFN $\lambda$  in infected hBMECs, ZIKV-infected hBMECs failed to secrete detectable or functional IFN $\beta$ / $\lambda$  and led us to hypothesize ZIKV post-transcriptionally inhibits IFN $\beta$ /IFN $\lambda$  expression (15).

ZIKV impairs IFN induction and IFN receptor responses through multiple mechanisms. ZIKV NS3/NS5, additional NS proteins, and sRNA reportedly suppress RIG-I/MDA-5 signaling pathway responses that induce IFN mRNA transcription (28–33). ZIKV also targets JAK/STAT signaling pathways downstream of IFNAR to restrict the induction of antiviral ISGs. NS2B3 degrades Jak kinase, preventing downstream STAT phosphorylation,

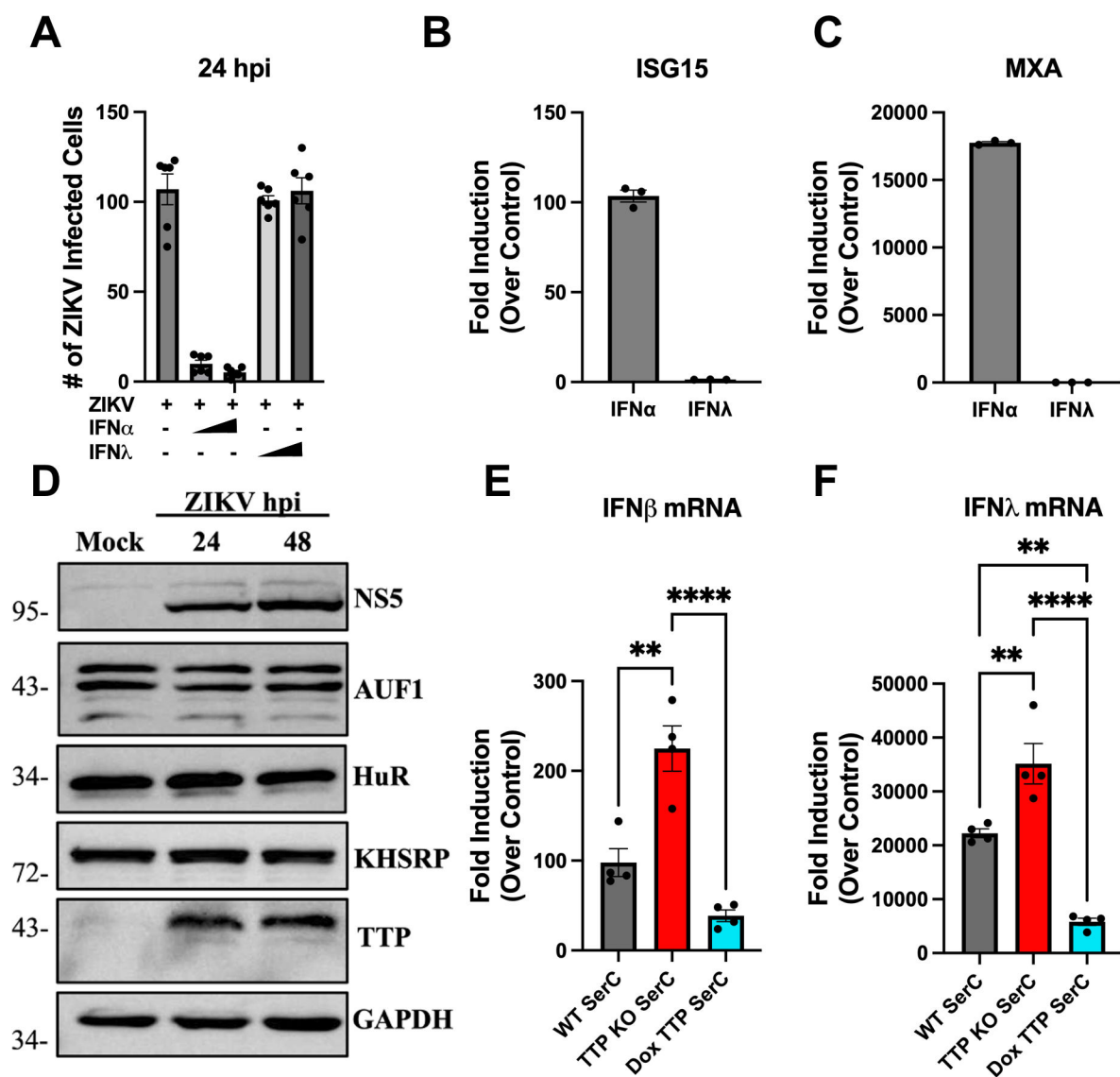


**FIG 8** TTP regulates IFN $\beta$ /IFN $\lambda$  expression in human Sertoli cells. (A through C) Primary hSerCs were ZIKV infected (MOI = 0.5) with or without IFN $\alpha$  (1,000 or 2,000 U/mL) or IFN $\lambda$  (10 or 50 ng/mL) addition. ZIKV antigen-positive hSerCs were quantified for 24 hpi using anti-DENV4 hyperimmune mouse ascitic fluid (A), and RNA was collected to assess ISG induction relative to untreated, uninfected WT hSerCs (B and C). (D) Primary hSerCs were ZIKV infected (MOI = 10), and lysates were analyzed for ARE-BP expression by Western blot. (E and F) Representative Western blot from two experiments. ZIKV-infected (MOI = 10) primary hSerCs, TTP KO-hSerCs, and TTP-expressing hSerCs were assayed for IFN $\beta$  (E) and IFN $\lambda$  (F) mRNAs for 24 hpi by qRT-PCR relative to WT, TTP KO, and Dox TTP uninfected control hSerCs. Data are presented as the mean  $\pm$  SEM; asterisks indicate statistical significance as determined by one-way ANOVA. \*\* $P \leq 0.002$ , \*\*\*\* $P \leq 0.0001$ . Experiments were performed at least three times unless otherwise noted.

while ZIKV NS5 inhibits STAT phosphorylation and promotes human STAT2 degradation (25, 28, 35, 36).

Despite ZIKV regulation of IFN induction, several reports note that IFN induction is dissociated from IFN secretion (9, 37, 39, 40). In ZIKV infected PBMCs IFN transcripts were induced, but PBMCs failed to secrete IFN $\alpha$  and IFN $\lambda$ , and ZIKV-infected placental macrophages, fetal neural progenitors, and dendritic cells similarly failed to secrete IFNs (9, 37, 39, 40). In dendritic cells, a comparison of IFN cDNA synthesis (hexamer versus oligo-dT) suggested IFN mRNA stability was unchanged by ZIKV infection, and translational IFN regulation was inferred (37). Collectively, IFN induction without IFN secretion following ZIKV infection was noted in immune cells, where TTP expression in response

to LPS is well characterized, and mirrored our own observations of ZIKV inhibiting IFN secretion in hBMECs at a translational level (9, 37, 39, 40).

ZIKV infection reportedly induces the expression of miRNAs that have been shown to regulate the production of ISGs, cell death, and chemotaxis and represent a potential mechanism of post-transcriptional IFN regulation (76–78). Although ZIKV induction of miRNAs targeting IFN $\beta$ /IFN $\lambda$  has not been reported, the distantly related *Flavivirus* hepatitis C virus (HCV) induces miRNAs targeting IFN $\lambda$  to restrain IFN signaling and promote viral persistence in hepatocytes (79, 80). We initially assessed miRNAs induced in ZIKV-infected hBMECs at 24 hpi but found no significant upregulation of canonical IFN targeting miRNAs (mir-34a, mir-145, or let-7b), with the IFN $\beta$  targeting miRNA, miR-34a, induced by only 1.61-fold ( $P$  value = 0.06) (81).

In HCV pathogenesis, IFN $\lambda$  ARE-mediated inhibition has been implicated. In the 3' UTR of *IFNL3*, an ARE polymorphism was identified that interfered with ARE sequence recognition, ultimately enhancing IFN $\lambda_3$  production and conferring cellular resistance to HCV (80, 82, 83). Both *IFNB1* and *IFNL1* transcripts produced by ZIKV-infected hBMECs contain AREs in their 3' UTRs (48, 84). This led us to hypothesize the AREs in IFN $\beta$ /IFN $\lambda$  mRNAs as targets of ZIKV post-transcriptional regulation and potential roles for ARE-BPs in ZIKV persistence in hBMECs. During ZIKV infection, ARE-BPs have primarily been observed as markers of stress granule localization but ARE-BPs as determinants of spread and persistence have remained understudied (85–87). Knockdown of HuR, an ARE-BP that stabilizes IFN mRNAs, was shown to increase ZIKV titers, although the effect on IFN expression was not assessed (42, 87).

Due to reports of ARE-BPs regulating IFN mRNAs, we assessed the expression and localization of TTP, KHSRP, AUF1, and HuR in ZIKV-infected hBMECs (41). We found that only TTP was induced by ZIKV infection and that TTP was localized to the cytoplasm. Importantly, ZIKV-directed TTP expression was independent of IRF3-directed IFN induction, and TTP was not induced in response to IFN addition to cells. How ZIKV triggers TTP induction independent of IRF3 is unclear and warrants further study but likely involves regulation by p38 MAPK. ZIKV infection reportedly activates p38 MAPK, a key regulator of LPS-directed TTP induction, activity, and protein stability (52, 62, 88, 89).

IFN regulation remains an understudied aspect of TTP biology and has not been addressed in the context of viral infections. Impaired IAV replication following TTP knockdown was attributed to an increase in COX-2 protein; however, the effect of TTP on IFN production was not assessed (67). Two studies have implicated IFN $\beta$  and IFN $\gamma$  as targets of TTP repression in LPS-treated murine macrophages and T cells, respectively; however, TTP regulation of IFN has not been assessed in virally infected, non-immune human cells (90, 91). We observed that TTP expression in hBMECs and Sertoli cells regulates IFN $\beta$ /IFN $\lambda$  mRNA abundance and protein expression in response to ZIKV infection. These cells comprise critical physiological barriers protecting brain and testicular tissues, respectively, and the ability to limit IFN responses likely fosters viral persistence and spread into these immune privileged compartments.

Apart from this study, the role of TTP in regulating IFN responses that restrict viral infection and spread in human cells has yet to be investigated, but TTP expression in a variety of cell types underscores its potential importance. In addition to TTP expression in brain, testicular, placental, and ovarian tissues, TTP is the most highly expressed in cervical tissue (92). IFN $\lambda$  secretion protects the female reproductive track and plays a critical role in preventing viral spread across placental barriers (93, 94). TTP expression by placental cells, including Hofbauer cells, has not been investigated; however, TTP expression may suppress IFN production by key mediators of ZIKV persistence to facilitate viral spread and congenital fetal infection. In these barrier settings, TTP-regulated IFN $\beta$ /IFN $\lambda$  responses are likely to be critical to ZIKV sexual transmission, persistence, and *in utero* spread to fetal tissues.

To determine if IFN $\beta$ /IFN $\lambda$  mRNA and secreted protein levels are altered due to TTP destabilization of IFN mRNAs, we assessed IFN $\beta$ , IFN $\lambda$ , and IL-6 degradation rates following addition of actinomycin D. The ability of TTP to promote IL-6 mRNA

degradation is well characterized in immune cells in response to LPS (69, 95). However, TTP regulation of IFNs is less clear with TTP overexpression enhancing IFN $\beta$  mRNA degradation 1 h, but not 4 h, post-LPS treatment, in murine bone marrow-derived macrophages (BMDMs) (91). In contrast, KO of a TTP activator, DUSP1, stabilized IFN $\beta$  mRNA only at 4 h post-LPS treatment, indicating that TTP interactions with IFN $\beta$  are temporally regulated (91).

TTP's ability to promote mRNA degradation is dependent on a complex and dynamic balance of phosphorylation and dephosphorylation events downstream of the MAPK signaling cascade and is largely mediated by p38 MAPK, MK2, DUSP1, and PP2A (60, 96). More investigation is required to fully characterize the phosphorylation status and expression of these TTP regulating proteins to determine how they influence TTP activity and transcript interaction during ZIKV infection. In TTP KO hBMECs, we observed no significant alteration to IFN $\beta$ /IFN $\lambda$  mRNA stability but did detect faster degradation of IL-6 mRNA. We assessed IFN mRNA stability at 24 hpi because it coincides with the peak of IFN induction and TTP expression following a synchronous ZIKV infection of hBMECs. However, we cannot discount altered IFN mRNA stability at other times post-infection, and it is unclear how IFN mRNA levels are enhanced during ZIKV infection of TTP KO cells. TTP also reportedly functions as a transcriptional co-repressor, inhibiting TNF- $\alpha$  promoter activity through interactions with NF- $\kappa$ B (60). TTP transcriptional repression of IFNs has not been investigated; however, we consider this regulation to be unlikely as it requires nuclear localization of TTP, which we did not observe during ZIKV infection of hBMECs (Fig. 2B). Ultimately, our findings are consistent with ZIKV-induced TTP repressing the translation of IFN $\beta$ /IFN $\lambda$  mRNAs to suppress IFN secretion.

TTP has multiple mechanisms of repressing ARE-mRNA translation and has been shown to directly form complexes with poly(A)-binding protein and the inhibitory eukaryotic initiation factor 4E2 (60, 61, 97). Recruitment of eIF4E2 to ARE-mRNAs prevented their association with eIF4E, a scaffold protein required for assembly of the translation initiation complex leading to the inhibition of cap-dependent translation (60, 61, 97). TTP also reportedly interacts with GYF2 to recruit the cap-binding translational repression complex 4EHP that competes for cap binding with eIF4E (59). However, the formation of translation regulating TTP complexes with IFN mRNAs and has not been addressed in endothelial cells, Sertoli cells, or trophoblasts that normally protect tissues from viral access (60, 61, 97).

Overall, our findings characterize a novel role for TTP in suppressing IFN $\beta$ /IFN $\lambda$  production in primary human BMECs and Sertoli cells in response to ZIKV infection. We found that TTP is induced by ZIKV independent of IRF3 and IFN activity, and that TTP post-transcriptionally inhibits IFN $\beta$ /IFN $\lambda$  protein expression and secretion despite transcriptional induction. These novel findings demonstrate that TTP regulation of IFN responses contributes to ZIKV spread and persistence and provides an additional mechanism for induced TTP to regulate IFN $\lambda$  expression, a critical determinant of ZIKV placental transmission (98). Our findings underscore the complexity of the IFN response to ZIKV and highlight a new post-transcriptional mechanism of innate immune interference that prevents IFN secretion and fosters ZIKV persistence and spread across key tissue barriers.

## MATERIALS AND METHODS

### Cells

C6/36 cells (ATCC CRL-1660) were grown in Dulbecco's modified Eagle's medium (DMEM) supplemented with 10% fetal bovine serum (FBS), penicillin (100  $\mu$ g/mL), streptomycin sulfate (100  $\mu$ g/mL), and amphotericin B (50  $\mu$ g/mL, Mediatech) at 28°C with 5% CO<sub>2</sub>. Human brain microvascular endothelial cells were purchased from Cell Biologics (H-6023) and grown in endothelial cell growth basal medium-2 with SingleQuots (Lonza) at 37°C in 5% CO<sub>2</sub>. hBMECs were discarded upon reaching passage 12. Human Sertoli cells were

purchased from ScienCell (#4520) and grown as above in Sertoli cell media (#4521). Vero E6 (ATCC CRL 1586), HEK293T (ATCC), and A549 (ATCC CCL-185) were grown in DMEM as above with 8% FBS.

## Virus

ZIKV (PRVABC59) was obtained from the ATCC (VR-1843) and passaged in C6/36 cells according to the manufacturer's instructions. Infectious ZIKV stocks ( $5 \times 10^5$  FFU/mL) were generated by inoculating confluent T75 flasks of C6/36 cells for 4 days in 2% DMEM before transfer to T175 flasks for 6 days prior to harvest and centrifugation of viral stock. Viral titers were determined by serial dilution and quantification of infected foci in Vero E6 cells for 24 hpi via immunoperoxidase staining with anti-DENV4 hyperimmune mouse ascitic fluid (ATCC), horseradish peroxidase-labeled anti-mouse IgG (1:2,000; KPL-074-1806), and 3-amino-9-ethylcarbazole. ZIKV infections were performed by absorbing virus onto primary hBMEC/hSerC monolayers ( $2\text{--}4 \times 10^5$  cells) for 2 h at 37°C, washing with phosphate-buffered saline (PBS), and resupplementing with media. For all experiments involving doxycycline induced, TTP-expressing hBMECs and hSerCs, 200-ng/mL doxycycline was maintained in culture media throughout the course of ZIKV infection.

## Induction and expression analysis

hBMECs ( $2 \times 10^5$ ) were ZIKV infected, transfected with 0.5- $\mu\text{g}/\text{mL}$  poly(I:C) and FuGENE 6 (1:3) or treated with 1,000 U/mL IFN $\alpha$  (Sigma) for 24 h prior to supernatant and RNA collection. For IFN and ISG induction experiments, IFN $\alpha$  (Sigma) and IFN $\lambda_1$  generated from IFN $\lambda_1$ -expressing HEK-293T cells were added to hBMEC/hSerCs/A549 concurrently with ZIKV (MOI = 0.5). Following inoculum removal, indicated concentrations of IFN $\alpha$ /IFN $\lambda_1$  were added back to monolayers before cell fixation or RNA collection for 24 hpi.

## Lentivirus, transduction, and selection

pLentiCRISPRv2 plasmid was purchased from Addgene (#52961), and gRNA was inserted as described previously (99, 100). pLV2CRISPR-hCas9:T2A: Puro-U6 was purchased from VectorBuilder for TTP KO. Lentivirus was produced in HEK 293 T cells following PEI transfection (5  $\mu\text{g}/1 \mu\text{g}$  DNA) of pLentiCRISPRv2, psPAX2 (Addgene #12260), and pLp/VSVG (Invitrogen) and was collected 5 days post-transfection. hBMECs were doubly transduced over 48 h and selected with puromycin (0.8  $\mu\text{g}/\text{mL}$ ) for 72 h prior to KO validation by Western blot. gRNAs used can be found in Table S1.

pCW57-MCS1-2A-MCS2 was purchased from Addgene (#71782) and used to conditionally express TTP and IFN $\lambda_1$  derived from ZIKV-infected hBMEC cDNA in the presence of doxycycline (0.2–1.0  $\mu\text{g}/\text{mL}$ ). TTP and IFN $\lambda_1$  were cloned using primers found in Table S1 and inserted between pCW57-MCS1-2A-MCS2 EcoRI (NEB #R3101S) and BamHI (NEB #R3136S) restriction sites.

## qRT-PCR analysis

RNA was purified using RNeasy Mini Kit (Qiagen) according to the manufacturer's instructions. cDNA was generated using Transcriptor first-strand cDNA synthesis kit (Roche) and ProtoScript II first-strand cDNA synthesis kit (New England BioLabs) using Oligo-p(dT)<sub>15</sub> or d(T)<sub>23</sub> VN primers. qRT-PCR primers used are found in Table S1.

cDNA was amplified using PerfeCTa SYBR Green SuperMix (QuantaBio) on a BioRad CFX96 Touch Real-Time PCR Detection System. All genes were normalized to internal  $\beta$ -actin controls, and gene induction was determined using  $2^{-\Delta\Delta Ct}$  over uninfected/uninduced controls of the same cell type. For mRNA half-life determination, hBMECs were treated with 5- $\mu\text{g}/\text{mL}$  actinomycin D (Sigma) for the indicated times prior to RNA purification. mRNA abundance over time was plotted relative to RNA collected imme-

diately following actinomycin addition and was assessed for significance via one-way analysis of variance using GraphPad Prism.

## ELISA

Levels of secreted IFN $\beta$  and IFN $\lambda$  in mock, ZIKV-infected, and poly (I:C)-treated supernatants were determined using DuoSet ELISA (R&D Systems) according to the manufacturer's instructions. ELISA plates (Immunolon 2, U-bottom; Dynatech Laboratories) were developed using tetramethylbenzidine, and optical density (O.D.) was measured using a Molecular Devices SpectraMax M5 plate reader (450 nm). Protein concentrations were calculated by fitting O.D. to a standard curve of purified IFN using SoftMax Pro software.

## Western blot analysis

Cells were washed in PBS prior to lysis on ice in buffer containing 1% NP-40, 0.1% SDS, 150 mM NaCl, 50 mM Tris-HCl pH 7.4, 2 mM EDTA, 10 nM NaF, 1 mM phenylmethylsulfonyl fluoride (PMSF), and protease inhibitor cocktail (Sigma). Protein concentration was determined using Pierce BCA Protein Assay Kit (Thermo) and 36  $\mu$ g of protein was resolved on a 10–12% SDS polyacrylamide gel. Proteins were transferred to a 0.4- $\mu$ m nitrocellulose membrane and blocked in either 5% bovine serum albumin or 5% non-fat milk prior to incubation with primary antibody. Cellular fractionation was performed as previously described (101). Antibodies used include ZIKV NS5 1:1,000 (GeneTex #GTX133327), AUF1 1:1,000 (Millipore 07–260), lamin B1 1:1,000 (Cell Signaling D4Q4Z), TTP 1:250 (Cell Signaling D113T), IRF3 1:1,000 (Cell Signaling D83B9), Myc 1:1,000 (Cell Signaling 2272S), KHSRP 1:1,000 (Cell Signaling E2E2U), HuR 1:1,000 (Santa Cruz sc-5261), and GAPDH 1:3,000 (Sigma G9545).

## Statistical analysis

Results in each figure were derived from data collected from  $\geq 3$  independent experiments and were displayed as the mean  $\pm$  standard error of the mean. One-way analysis of variance, two-way analysis of variance, and unpaired Student's *t* test were used where indicated, with *P* values of  $\leq 0.05$  considered significant. All statistical tests were performed using GraphPad Prism version 9.

## ACKNOWLEDGMENTS

We thank Patrick Hearing, Nancy Reich-Marshall, Laurie Krug, Daniel Salamango, Elena Gorbunova, and William A. Schutt, Jr., for their helpful discussions and manuscript feedback.

This work was supported by funding from a DOD TBDRP Idea Development Award (W81XWH2210702), National Institutes of Health grants (NIAID R01AI12901005, R21AI13173902, and T32AI007539), and a Stony Brook University Seed grant. The funders had no role in study design, data collection, and interpretation or the decision to submit the work for publication.

We declare no conflict of interest.

## AUTHOR AFFILIATIONS

<sup>1</sup>Department of Microbiology and Immunology, Stony Brook University, Stony Brook, New York, USA

<sup>2</sup>Center for Infectious Disease, Stony Brook University, Stony Brook, New York, USA

<sup>3</sup>Molecular and Cell Biology Program, Stony Brook University, Stony Brook, New York, USA

## AUTHOR ORCIDs

Erich R. Mackow  <http://orcid.org/0000-0001-9156-1222>

## FUNDING

Funder	Grant(s)	Author(s)
U.S. Department of Defense (DOD)	W81XWH2210702	Erich R. Mackow
HHS   NIH   National Institute of Allergy and Infectious Diseases (NIAID)	R01AI12901005	Erich R. Mackow
HHS   NIH   National Institute of Allergy and Infectious Diseases (NIAID)	R21AI13173902	Erich R. Mackow
HHS   NIH   National Institute of Allergy and Infectious Diseases (NIAID)	T32AI007539	Megan C. Mladinich

## AUTHOR CONTRIBUTIONS

William R. Schutt, Conceptualization, Data curation, Formal analysis, Investigation, Methodology, Resources, Software, Supervision, Validation, Visualization, Writing – original draft, Writing – review and editing | Jonas N. Conde, Conceptualization, Data curation, Investigation, Methodology | Megan C. Mladinich, Conceptualization, Investigation, Methodology | Grace E. Himmler, Conceptualization, Investigation, Methodology, Writing – review and editing | Erich R. Mackow, Conceptualization, Data curation, Formal analysis, Funding acquisition, Investigation, Methodology, Project administration, Resources, Supervision, Validation, Writing – original draft, Writing – review and editing

## DIRECT CONTRIBUTION

This article is a direct contribution from Erich R. Mackow, a Fellow of the American Academy of Microbiology, who arranged for and secured reviews by Aaron Carlin, University of California-San Diego School of Medicine, and Michael Buchmeier, University of California, Irvine.

## ADDITIONAL FILES

The following material is available [online](#).

### Supplemental Material

**Supplemental Figure Legends (mBio01742-23-s0001.docx).** Legends to Table S1 and Fig. S1 to 4.

**Figure S1 (mBio01742-23-s0002.tif).** IFN $\alpha$ / $\lambda$  induce ISGs in A549 cells.

**Figure S2 (mBio01742-23-s0003.tif).** ZIKV induction of MXA, IFIT1, and CCL5 is IRF3 dependent.

**Figure S3 (mBio01742-23-s0004.tif).** Validation of hBMEC TTP KO and doxycycline-induced TTP expression.

**Figure S4 (mBio01742-23-s0005.tif).** Validation of hSerC TTP KO and doxycycline-induced TTP expression.

**Table S1 (mBio01742-23-s0006.tif).** Oligonucleotide primers.

## REFERENCES

1. Miner JJ, Cao B, Govero J, Smith AM, Fernandez E, Cabrera OH, Garber C, Noll M, Klein RS, Noguchi KK, Mysorekar IU, Diamond MS. 2016. Zika virus infection during pregnancy in mice causes placental damage and fetal demise. *Cell* 165:1081–1091. <https://doi.org/10.1016/j.cell.2016.05.008>
2. Calvet G, Aguiar RS, Melo ASO, Sampaio SA, de Filippis I, Fabri A, Araujo ESM, de Sequeira PC, de Mendonça MCL, de Oliveira L, Tschoeke DA, Schrago CG, Thompson FL, Brasil P, Dos Santos FB, Nogueira RMR, Tanuri A, de Filippis AMB. 2016. Detection and sequencing of Zika virus from amniotic fluid of fetuses with microcephaly in Brazil: a case study. *Lancet Infect Dis* 16:653–660. [https://doi.org/10.1016/S1473-3099\(16\)00095-5](https://doi.org/10.1016/S1473-3099(16)00095-5)
3. Campos R de M, Cirne-Santos C, Meira GLS, Santos LLR, de Meneses MD, Friedrich J, Jansen S, Ribeiro MS, da Cruz IC, Schmidt-Chanasit J, Ferreira DF. 2016. Prolonged detection of Zika virus RNA in urine samples during the ongoing Zika virus epidemic in Brazil. *J Clin Virol* 77:69–70. <https://doi.org/10.1016/j.jcv.2016.02.009>
4. Vesnaver TV, Tul N, Mehrabi S, Parisson F, Štrafela P, Mlakar J, Pižem J, Korva M, Zupanc TA, Popović M. 2017. Zika virus associated microcephaly/micrencephaly-fetal brain imaging in comparison with neuropathology. *BJOG* 124:521–525. <https://doi.org/10.1111/1471-0528.14423>



5. Paz-Bailey G, Rosenberg ES, Sharp TM. 2019. Persistence of Zika virus in body fluids - final report. *N Engl J Med* 380:198–199. <https://doi.org/10.1056/NEJMc1814416>
6. Hygino da Cruz LC Jr, Nascimento OJM, Lopes FPPL, da Silva IRF. 2018. Neuroimaging findings of Zika virus-associated neurologic complications in adults. *AJNR Am J Neuroradiol* 39:1967–1974. <https://doi.org/10.3174/ajnr.A5649>
7. Mead PS, Hills SL, Brooks JT. 2018. Zika virus as a sexually transmitted pathogen. *Curr Opin Infect Dis* 31:39–44. <https://doi.org/10.1097/QCO.0000000000000414>
8. de Noronha L, Zanluca C, Burger M, Suzukawa AA, Azevedo M, Rebutini PZ, Novadzki IM, Tanabe LS, Presibella MM, Duarte Dos Santos CN. 2018. Zika virus infection at different pregnancy stages: anatomopathological findings, target cells and viral persistence in placental tissues. *Front Microbiol* 9:2266. <https://doi.org/10.3389/fmicb.2018.02266>
9. Quicke KM, Bowen JR, Johnson EL, McDonald CE, Ma H, O'Neal JT, Rajakumar A, Wrammert J, Rimawi BH, Pulendran B, Schinazi RF, Chakraborty R, Suthar MS. 2016. Zika virus infects human placental macrophages. *Cell Host & Microbe* 20:83–90. <https://doi.org/10.1016/j.chom.2016.05.015>
10. Tang H, Hammack C, Ogden SC, Wen Z, Qian X, Li Y, Yao B, Shin J, Zhang F, Lee EM, Christian KM, Didier RA, Jin P, Song H, Ming G. 2016. Zika virus infects human cortical neural progenitors and attenuates their growth. *Cell Stem Cell* 18:587–590. <https://doi.org/10.1016/j.stem.2016.02.016>
11. Zhou K, Wang L, Yu D, Huang H, Ji H, Mo X. 2017. Molecular and cellular insights into Zika virus-related neuropathies. *J Neurovirol* 23:341–346. <https://doi.org/10.1007/s13365-017-0514-3>
12. Goasdoué K, Miller SM, Colditz PB, Björkman ST. 2017. Review: the blood-brain barrier; protecting the developing fetal brain. *Placenta* 54:111–116. <https://doi.org/10.1016/j.placenta.2016.12.005>
13. Teixeira FME, Pietrobon AJ, Oliveira L de M, Oliveira L da S, Sato MN. 2020. Maternal-fetal interplay in Zika virus infection and adverse perinatal outcomes. *Front Immunol* 11:175. <https://doi.org/10.3389/fimmu.2020.00175>
14. Noronha L de, Zanluca C, Azevedo MLV, Luz KG, Santos CNDD. 2016. Zika virus damages the human placental barrier and presents marked fetal neurotropism. *Mem Inst Oswaldo Cruz* 111:287–293. <https://doi.org/10.1590/0074-02760160085>
15. Mladinich MC, Schwedes J, Mackow ER. 2017. Zika virus persistently infects and is basolaterally released from primary human brain microvascular endothelial cells. *mBio* 8:e00952-17. <https://doi.org/10.1128/mBio.00952-17>
16. Conde JN, Schutt WR, Mladinich M, Sohn S-Y, Hearing P, Mackow ER. 2020. NS5 Sumoylation directs nuclear responses that permit Zika virus to persistently infect human brain microvascular endothelial cells. *J Virol* 94:e01086-20. <https://doi.org/10.1128/JVI.01086-20>
17. Mladinich MC, Conde JN, Schutt WR, Sohn S-Y, Mackow ER, Coyne CB. 2021. Blockade of Autocrine Ccl5 responses inhibits Zika virus persistence and spread in human brain Microvascular endothelial cells. *mBio* 12. <https://doi.org/10.1128/mBio.01962-21>
18. Kumar A, Jovel J, Lopez-Orozco J, Limonta D, Airo AM, Hou S, Stryapunina I, Fibke C, Moore RB, Hobman TC. 2018. Human Sertoli cells support high levels of Zika virus replication and persistence. *Sci Rep* 8:5477. <https://doi.org/10.1038/s41598-018-23899-x>
19. Siemann DN, Strange DP, Maharaj PN, Shi P-Y, Verma S. 2017. Zika virus infects human Sertoli cells and modulates the integrity of the *In Vitro* blood-testis barrier model. *J Virol* 91:e00623-17. <https://doi.org/10.1128/JVI.00623-17>
20. Pober JS, Sessa WC. 2007. Evolving functions of endothelial cells in inflammation. *Nat Rev Immunol* 7:803–815. <https://doi.org/10.1038/nri2171>
21. Mai J, Virtue A, Shen J, Wang H, Yang XF. 2013. An evolving new paradigm: endothelial cells--conditional innate immune cells. *J Hematol Oncol* 6:61. <https://doi.org/10.1186/1756-8722-6-61>
22. Marshall EM, Koopmans MPG, Rockx B. 2022. A journey to the central nervous system: routes of flaviviral neuroinvasion in human disease. *Viruses* 14:2096. <https://doi.org/10.3390/v14102096>
23. Conde JN, Sanchez-Vicente S, Saladino N, Gorbunova EE, Schutt WR, Mladinich MC, Himmler GE, Benach J, Kim HK, Mackow ER. 2022. Powassan viruses spread cell to cell during direct isolation from *Ixodes* ticks and persistently infect human brain endothelial cells and pericytes. *J Virol* 96:e0168221. <https://doi.org/10.1128/JVI.01682-21>
24. Dalrymple NA, Mackow ER. 2012. Endothelial cells elicit immune-enhancing responses to dengue virus infection. *J Virol* 86:6408–6415. <https://doi.org/10.1128/JVI.00213-12>
25. Kumar A, Hou S, Airo AM, Limonta D, Mancinelli V, Branton W, Power C, Hobman TC. 2016. Zika virus inhibits type-I interferon production and downstream signaling. *EMBO Rep* 17:1766–1775. <https://doi.org/10.15252/embr.201642627>
26. Samuel MA, Diamond MS. 2005. Alpha/beta interferon protects against lethal West Nile virus infection by restricting cellular tropism and enhancing neuronal survival. *J Virol* 79:13350–13361. <https://doi.org/10.1128/JVI.79.21.13350-13361.2005>
27. Rashid M-U, Zahedi-Amiri A, Glover KKM, Gao A, Nickol ME, Kindrachuk J, Wilkins JA, Coombs KM. 2020. Zika virus dysregulates human Sertoli cell proteins involved in spermatogenesis with little effect on tight junctions. *PLoS Negl Trop Dis* 14:e0008335. <https://doi.org/10.1371/journal.pntd.0008335>
28. Lee LJ, Komarasamy TV, Adnan NAA, James W, Rmt Balasubramaniam V. 2021. Hide and seek: the interplay between Zika virus and the host immune response. *Front Immunol* 12:750365. <https://doi.org/10.3389/fimmu.2021.750365>
29. Hertzog J, Dias Junior AG, Rigby RE, Donald CL, Mayer A, Sezgin E, Song C, Jin B, Hublitz P, Eggeling C, Kohl A, Rehwinkel J. 2018. Infection with a Brazilian isolate of Zika virus generates RIG-I stimulatory RNA and the viral NS5 protein blocks type I IFN induction and signaling. *Eur J Immunol* 48:1120–1136. <https://doi.org/10.1002/eji.201847483>
30. Li W, Li N, Dai S, Hou G, Guo K, Chen X, Yi C, Liu W, Deng F, Wu Y, Cao X. 2019. Zika virus circumvents host innate immunity by targeting the adaptor proteins MAVS and MITA. *FASEB J* 33:9929–9944. <https://doi.org/10.1096/fj.201900260R>
31. Schilling M, Bridgeman A, Gray N, Hertzog J, Hublitz P, Kohl A, Rehwinkel J. 2020. RIG-I plays a dominant role in the induction of transcriptional changes in Zika virus-infected cells, which protect from virus-induced cell death. *Cells* 9:1476. <https://doi.org/10.3390/cells9061476>
32. Donald CL, Brennan B, Cumberworth SL, Rezelj VV, Clark JJ, Cordeiro MT, Freitas de Oliveira França R, Pena LJ, Wilkie GS, Da Silva Filipe A, Davis C, Hughes J, Varjak M, Selinger M, Zuvanov L, Owsianka AM, Patel AH, McLauchlan J, Lindenbach BD, Fall G, Sall AA, Biek R, Rehwinkel J, Schmetzler E, Kohl A, Morrison AC. 2016. Full genome sequence and sfRNA interferon antagonist activity of Zika virus from Recife. *PLoS Negl Trop Dis* 10:e0005048. <https://doi.org/10.1371/journal.pntd.0005048>
33. Göertz GP, Abbo SR, Fros JJ, Pijlman GP. 2018. Functional RNA during Zika virus infection. *Virus Research* 254:41–53. <https://doi.org/10.1016/j.virusres.2017.08.015>
34. Michalski D, Ontiveros JG, Russo J, Charley PA, Anderson JR, Heck AM, Geiss BJ, Wilusz J. 2019. Zika virus noncoding sfRNAs sequester multiple host-derived RNA-binding proteins and modulate mRNA decay and splicing during infection. *J Biol Chem* 294:16282–16296. <https://doi.org/10.1074/jbc.RA119.009129>
35. Wu Y, Liu Q, Zhou J, Xie W, Chen C, Wang Z, Yang H, Cui J. 2017. Zika virus evades interferon-mediated antiviral response through the co-operation of multiple nonstructural proteins *in vitro*. *Cell Discov* 3:17006. <https://doi.org/10.1038/celldisc.2017.6>
36. Carlin AF, Vizcarra EA, Branche E, Viramontes KM, Suarez-Amaran L, Ley K, Heinz S, Benner C, Shresta S, Glass CK. 2018. Deconvolution of pro- and antiviral genomic responses in Zika virus-infected and bystander macrophages. *Proc Natl Acad Sci U S A* 115:E9172–E9181. <https://doi.org/10.1073/pnas.1807690115>
37. Bowen JR, Quicke KM, Maddur MS, O'Neal JT, McDonald CE, Fedorova NB, Puri V, Shabman RS, Pulendran B, Suthar MS. 2017. Zika virus antagonizes type I interferon responses during infection of human dendritic cells. *PLoS Pathog* 13:e1006164. <https://doi.org/10.1371/journal.ppat.1006164>
38. Papa MP, Meuren LM, Coelho SVA, Lucas CG de O, Mustafá YM, Lemos Matassoli F, Silveira PP, Frost PS, Pezzuto P, Ribeiro MR, Tanuri A, Nogueira ML, Campanati L, Bozza MT, Paula Neto HA, Pimentel-Coelho PM, Figueiredo CP, de Aguiar RS, de Arruda LB. 2017. Zika virus infects, activates, and crosses brain microvascular endothelial cells, without

- barrier disruption. *Front Microbiol* 8:2557. <https://doi.org/10.3389/fmicb.2017.02557>
39. Colavita F, Bordoni V, Caglioti C, Biava M, Castilletti C, Bordi L, Quartu S, Iannetta M, Ippolito G, Agrati C, Capobianchi MR, Lalle E. 2018. ZIKV infection induces an inflammatory response but fails to activate types I, II, and III IFN response in human PBMC. *Mediators Inflamm* 2018:2450540. <https://doi.org/10.1155/2018/2450540>
  40. Hanners NW, Eitson JL, Usui N, Richardson RB, Wexler EM, Konopka G, Schoggins JW. 2016. Western Zika virus in human fetal neural progenitors persists long term with partial cytopathic and limited immunogenic effects. *Cell Rep* 15:2315–2322. <https://doi.org/10.1016/j.celrep.2016.05.075>
  41. Khabar KSA, Young HA. 2007. Post-transcriptional control of the interferon system. *Biochimie* 89:761–769. <https://doi.org/10.1016/j.biochi.2007.02.008>
  42. Herdy B, Karonitsch T, Vladimer GI, Tan CSH, Stukalov A, Trefzer C, Bigenzahn JW, Theil T, Holinka J, Kiener HP, Colinge J, Bennett KL, Superti-Furga G. 2015. The RNA-binding protein HuR/ELAVL1 regulates IFN- $\beta$  mRNA abundance and the type I IFN response. *Eur J Immunol* 45:1500–1511. <https://doi.org/10.1002/eji.201444979>
  43. Barreau C, Paillard L, Osborne HB. 2005. AU-rich elements and associated factors: are there unifying principles *Nucleic Acids Res* 33:7138–7150. <https://doi.org/10.1093/nar/gki1012>
  44. Pasté M, Huez G, Krus V. 2003. Deadenylation of interferon- $\beta$  mRNA is mediated by both the AU-rich element in the 3'-untranslated region and an instability sequence in the coding region. *Eur J Biochem* 270:1590–1597. <https://doi.org/10.1046/j.1432-1033.2003.03530.x>
  45. Schmidtke L, Schrick K, Saurin S, Käfer R, Gather F, Weinmann-Menke J, Kleinert H, Pautz A. 2019. The KH-type splicing regulatory protein (KSRP) regulates type III interferon expression post-transcriptionally. *Biochem J* 476:333–352. <https://doi.org/10.1042/BCJ20180522>
  46. Lin WJ, Zheng X, Lin CC, Tsao J, Zhu X, Cody JJ, Coleman JM, Gherzi R, Luo M, Townes TM, Parker JN, Chen CY. 2011. Posttranscriptional control of type I interferon genes by KSRP in the innate immune response against viral infection. *Mol Cell Biol* 31:3196–3207. <https://doi.org/10.1128/MCB.05073-11>
  47. King PH, Chen CY. 2014. Role of KSRP in control of type I interferon and cytokine expression. *J Interferon Cytokine Res* 34:267–274. <https://doi.org/10.1089/jir.2013.0143>
  48. Savan R. 2014. Post-transcriptional regulation of interferons and their signaling pathways. *J Interferon Cytokine Res* 34:318–329. <https://doi.org/10.1089/jir.2013.0117>
  49. Chamboredon S, Ciaïa D, Desroches-Castan A, Savi P, Bono F, Feige J-J, Cherradi N. 2011. Hypoxia-inducible factor-1 $\alpha$  mRNA: a new target for destabilization by tristetraprolin in endothelial cells. *Mol Biol Cell* 22:3366–3378. <https://doi.org/10.1091/mbc.E10-07-0617>
  50. Zhang H, Taylor WR, Joseph G, Caracciolo V, Gonzales DM, Sidell N, Seli E, Blackshear PJ, Kallen CB. 2013. mRNA-binding protein ZFP36 is expressed in atherosclerotic lesions and reduces inflammation in aortic endothelial cells. *Arterioscler Thromb Vasc Biol* 33:1212–1220. <https://doi.org/10.1161/ATVBAHA.113.301496>
  51. Brooks SA, Blackshear PJ. 2013. Tristetraprolin (TTP): interactions with mRNA and proteins, and current thoughts on mechanisms of action. *Biochim Biophys Acta* 1829:666–679. <https://doi.org/10.1016/j.bbaggm.2013.02.003>
  52. Kovarik P, Bestehorn A, Fesselet J. 2021. Conceptual advances in control of inflammation by the RNA-binding protein tristetraprolin. *Front Immunol* 12:751313. <https://doi.org/10.3389/fimmu.2021.751313>
  53. Carreño A, Lykke-Andersen J. 2022. The conserved CNOT1 interaction motif of tristetraprolin regulates ARE-mRNA decay independently of the p38 MAPK-MK2 kinase pathway. *Mol Cell Biol* 42:e0005522. <https://doi.org/10.1128/mcb.00055-22>
  54. Clement SL, Scheckel C, Stoecklin G, Lykke-Andersen J. 2011. Phosphorylation of tristetraprolin by MK2 impairs AU-rich element mRNA decay by preventing deadenylase recruitment. *Mol Cell Biol* 31:256–266. <https://doi.org/10.1128/MCB.00717-10>
  55. Sandler H, Kreth J, Timmers HTM, Stoecklin G. 2011. Not1 mediates recruitment of the deadenylase Caf1 to mRNAs targeted for degradation by tristetraprolin. *Nucleic Acids Res* 39:4373–4386. <https://doi.org/10.1093/nar/gkr011>
  56. Fabian MR, Frank F, Rouya C, Siddiqui N, Lai WS, Karetnikov A, Blackshear PJ, Nagar B, Sonenberg N. 2013. Structural basis for the recruitment of the human CCR4-NOT deadenylase complex by tristetraprolin. *Nat Struct Mol Biol* 20:735–739. <https://doi.org/10.1038/nsmb.2572>
  57. Fenger-Grøn M, Fillman C, Norrild B, Lykke-Andersen J. 2005. Multiple processing body factors and the ARE binding protein TTP activate mRNA decapping. *Mol Cell* 20:905–915. <https://doi.org/10.1016/j.molcel.2005.10.031>
  58. Qi MY, Wang ZZ, Zhang Z, Shao Q, Zeng A, Li XQ, Li WQ, Wang C, Tian FJ, Li Q, Zou J, Qin YW, Brewer G, Huang S, Jing Q. 2012. AU-rich-element-dependent translation repression requires the cooperation of tristetraprolin and RCK/P54. *Mol Cell Biol* 32:913–928. <https://doi.org/10.1128/MCB.05340-11>
  59. Fu R, Olsen MT, Webb K, Bennett EJ, Lykke-Andersen J. 2016. Recruitment of the 4EHP-GYF2 cap-binding complex to tetraproline motifs of tristetraprolin promotes repression and degradation of mRNAs with AU-rich elements. *RNA* 22:373–382. <https://doi.org/10.1261/rna.054833.115>
  60. Rodríguez-Gómez G, Paredes-Villa A, Cervantes-Badillo MG, Gómez-Sonora JP, Jorge-Pérez JH, Cervantes-Roldán R, León-Del-Río A. 2021. Tristetraprolin: a cytosolic regulator of mRNA turnover moonlighting as transcriptional corepressor of gene expression. *Mol Genet Metab* 133:137–147. <https://doi.org/10.1016/j.ymgme.2021.03.015>
  61. Tao X, Gao G. 2015. Tristetraprolin recruits eukaryotic initiation factor 4E2 to repress translation of AU-rich element-containing mRNAs. *Mol Cell Biol* 35:3921–3932. <https://doi.org/10.1128/MCB.00845-15>
  62. Rappl P, Brüne B, Schmid T. 2021. Role of tristetraprolin in the resolution of inflammation. *Biology* 10:66. <https://doi.org/10.3390/biology10010066>
  63. Chang W-L, Tarn W-Y. 2009. A role for transportin in deposition of TTP to cytoplasmic RNA granules and mRNA decay. *Nucleic Acids Res* 37:6600–6612. <https://doi.org/10.1093/nar/gkp717>
  64. Chou C-F, Lin W-J, Lin C-C, Lubber CA, Godbout R, Mann M, Chen C-Y. 2013. DEAD box protein DDX1 regulates cytoplasmic localization of KSRP. *PLoS One* 8:e73752. <https://doi.org/10.1371/journal.pone.0073752>
  65. Blaxall BC, Dwyer-Nield LD, Bauer AK, Bohlmeyer TJ, Malkinson AM, Port JD. 2000. Differential expression and localization of the mRNA binding proteins, AU-rich element mRNA binding protein (AUF1). *Mol Carcinog* 28:76–83. [https://doi.org/10.1002/1098-2744\(200006\)28:2<76::AID-MC3>3.0.CO;2-0](https://doi.org/10.1002/1098-2744(200006)28:2<76::AID-MC3>3.0.CO;2-0)
  66. Smallie T, Ross EA, Ammit AJ, Cunliffe HE, Tang T, Rosner DR, Ridley ML, Buckley CD, Saklatvala J, Dean JL, Clark AR. 2015. Dual-specificity phosphatase 1 and tristetraprolin cooperate to regulate macrophage responses to lipopolysaccharide. *J Immunol* 195:277–288. <https://doi.org/10.4049/jimmunol.1402830>
  67. Dudek SE, Nitzsche K, Ludwig S, Ehrhardt C. 2016. Influenza A viruses suppress cyclooxygenase-2 expression by affecting its mRNA stability. *Sci Rep* 6:27275. <https://doi.org/10.1038/srep27275>
  68. Lin R, Mamane Y, Hiscott J. 1999. Structural and functional analysis of interferon regulatory factor 3: localization of the transactivation and autoinhibitory domains. *Mol Cell Biol* 19:2465–2474. <https://doi.org/10.1128/MCB.19.4.2465>
  69. Zhao W, Liu M, D'Silva NJ, Kirkwood KL. 2011. Tristetraprolin regulates interleukin-6 expression through P38 MAPK-dependent affinity changes with mRNA 3' untranslated region. *J Interferon Cytokine Res* 31:629–637. <https://doi.org/10.1089/jir.2010.0154>
  70. Cheng CY, Mruk DD. 2012. The blood-testis barrier and its implications for male contraception. *Pharmacol Rev* 64:16–64. <https://doi.org/10.1124/pr.110.002790>
  71. Paz-Bailey G, Rosenberg ES, Doyle K, Munoz-Jordan J, Santiago GA, Klein L, Perez-Padilla J, Medina FA, Waterman SH, Gubern CG, Alvarado LI, Sharp TM. 2018. Persistence of Zika virus in body fluids preliminary report. *N Engl J Med* 379:1234–1243. <https://doi.org/10.1056/NEJMoa1613108>
  72. Miner JJ, Diamond MS. 2017. Zika virus pathogenesis and tissue tropism. *Cell Host Microbe* 21:134–142. <https://doi.org/10.1016/j.chom.2017.01.004>

73. Hong S, Van Kaer L. 1999. Immune privilege: keeping an eye on natural killer T cells. *J Exp Med* 190:1197–1200. <https://doi.org/10.1084/jem.190.9.1197>
74. Ding J, Aldo P, Roberts CM, Stabach P, Liu H, You Y, Qiu X, Jeong J, Maxwell A, Lindenbach B, Braddock D, Liao A, Mor G. 2021. Placenta-derived interferon-stimulated gene 20 controls ZIKA virus infection. *EMBO Rep* 22:e52450. <https://doi.org/10.15252/embr.202152450>
75. Aagaard KM, Lahon A, Suter MA, Arya RP, Seferovic MD, Vogt MB, Hu M, Stossi F, Mancini MA, Harris RA, Kahr M, Eppes C, Rac M, Belfort MA, Park CS, Lacorazza D, Rico-Hesse R. 2017. Primary human placental trophoblasts are permissive for Zika virus (ZIKV) replication. *Sci Rep* 7:41389. <https://doi.org/10.1038/srep41389>
76. Seong RK, Lee JK, Cho GJ, Kumar M, Shin OS. 2020. mRNA and miRNA profiling of Zika virus-infected human umbilical cord mesenchymal stem cells identifies miR-142-5p as an antiviral factor. *Emerg Microbes Infect* 9:2061–2075. <https://doi.org/10.1080/22221751.2020.1821581>
77. Fernandez GJ, Ramírez-Mejía JM, Urcuqui-Inchima S. 2022. Transcriptional and post-transcriptional mechanisms that regulate the genetic program in Zika virus-infected human umbilical cord mesenchymal stem cells. *Int J Biochem Cell Biol* 153:106312. <https://doi.org/10.1016/j.biocel.2022.106312>
78. Polonio CM, da Silva P, Russo FB, Hyppolito BRN, Zanluqui NG, Benazzato C, Beltrão-Braga PCB, Muxel SM, Peron JPS. 2022. microRNAs control antiviral immune response, cell death and chemotaxis pathways in human neuronal precursor cells (NPCs) during Zika virus infection. *Int J Mol Sci* 23:10282. <https://doi.org/10.3390/ijms231810282>
79. Jarret A, McFarland AP, Horner SM, Kell A, Schwerk J, Hong M, Badil S, Joslyn RC, Baker DP, Carrington M, Hagedorn CH, Gale M, Savan R. 2016. Hepatitis-C-virus-induced microRNAs dampen interferon-mediated antiviral signaling. *Nat Med* 22:1475–1481. <https://doi.org/10.1038/nm.4211>
80. McFarland AP, Horner SM, Jarret A, Joslyn RC, Bindewald E, Shapiro BA, Delker DA, Hagedorn CH, Carrington M, Gale M, Savan R. 2014. The favorable *IFNL3* genotype escapes mRNA decay mediated by AU-rich elements and hepatitis C virus-induced microRNAs. *Nat Immunol* 15:72–79. <https://doi.org/10.1038/ni.2758>
81. Witwer KW, Sisk JM, Gama L, Clements JE. 2010. MicroRNA regulation of IFN- $\beta$  protein expression: rapid and sensitive modulation of the innate immune response. *J Immunol* 184:2369–2376. <https://doi.org/10.4049/jimmunol.0902712>
82. Ge D, Fellay J, Thompson AJ, Simon JS, Shianna KV, Urban TJ, Heinzen EL, Qiu P, Bertelsen AH, Muir AJ, Sulkowski M, McHutchison JG, Goldstein DB. 2009. Genetic variation in *IL28B* predicts hepatitis C treatment-induced viral clearance. *Nature* 461:399–401. <https://doi.org/10.1038/nature08309>
83. Suppiah V, Moldovan M, Ahlenstiel G, Berg T, Weltman M, Abate ML, Bassendine M, Spengler U, Dore GJ, Powell E, Riordan S, Sheridan D, Smedile A, Fragomeli V, Müller T, Bahlo M, Stewart GJ, Booth DR, George J. 2009. *IL28B* is associated with response to chronic hepatitis C interferon- $\alpha$  and ribavirin therapy. *Nat Genet* 41:1100–1104. <https://doi.org/10.1038/ng.447>
84. Sedlyarov V, Fallmann J, Ebner F, Huemer J, Sneezum L, Ivin M, Kreiner K, Tanzer A, Vogl C, Hofacker I, Kovarik P. 2016. Tristetraprolin binding site atlas in the macrophage transcriptome reveals a switch for inflammation resolution. *Mol Syst Biol* 12:868. <https://doi.org/10.15252/msb.20156628>
85. Hou S, Kumar A, Xu Z, Airo AM, Stryapunina I, Wong CP, Branton W, Tchesnokov E, Götte M, Power C, Hobman TC, Diamond MS. 2017. Zika virus hijacks stress granule proteins and modulates the host stress response. *J Virol* 91. <https://doi.org/10.1128/JVI.00474-17>
86. Amorim R, Temzi A, Griffin BD, Moulard AJ. 2017. Zika virus inhibits eIF2 $\alpha$ -dependent stress granule assembly. *PLoS Negl Trop Dis* 11:e0005775. <https://doi.org/10.1371/journal.pntd.0005775>
87. Bonenfant G, Williams N, Netzband R, Schwarz MC, Evans MJ, Pager CT. 2019. Zika virus subverts stress granules to promote and restrict viral gene expression. *J Virol* 93:e00520-19. <https://doi.org/10.1128/JVI.00520-19>
88. Mikkelsen SS, Jensen SB, Chiliveru S, Melchjorsen J, Julkunen I, Gaestel M, Arthur JSC, Flavell RA, Ghosh S, Paludan SR. 2009. RIG-I-mediated activation of p38 MAPK is essential for viral induction of interferon and activation of dendritic cells: dependence on TRAF2 and TAK1. *J Biol Chem* 284:10774–10782. <https://doi.org/10.1074/jbc.M807272200>
89. Zhu S, Luo H, Liu H, Ha Y, Mays ER, Lawrence RE, Winkelmann E, Barrett AD, Smith SB, Wang M, Wang T, Zhang W. 2017. p38MAPK plays a critical role in induction of a pro-inflammatory phenotype of retinal muller cells following Zika virus infection. *Antiviral Res* 145:70–81. <https://doi.org/10.1016/j.antiviral.2017.07.012>
90. Ogilvie RL, Sternjohn JR, Rattenbacher B, Vlasova IA, Williams DA, Hau HH, Blackshear PJ, Bohjanen PR. 2009. Tristetraprolin mediates interferon- $\gamma$  mRNA decay. *J Biol Chem* 284:11216–11223. <https://doi.org/10.1074/jbc.M901229200>
91. McGuire VA, Rosner D, Ananieva O, Ross EA, Elcombe SE, Naqvi S, van den Bosch MMW, Monk CE, Ruiz-Zorrilla Diez T, Clark AR, Arthur JSC. 2017. Beta interferon production is regulated by p38 mitogen-activated protein kinase in macrophages via both MSK1/2- and tristetraprolin-dependent pathways. *Mol Cell Biol* 37:e00454-16. <https://doi.org/10.1128/MCB.00454-16>
92. Carrick DM, Blackshear PJ. 2007. Comparative expression of tristetraprolin (TTP) family member transcripts in normal human tissues and cancer cell lines. *Arch Biochem Biophys* 462:278–285. <https://doi.org/10.1016/j.abb.2007.04.011>
93. Caine EA, Scheaffer SM, Arora N, Zaitsev K, Artyomov MN, Coyne CB, Moley KH, Diamond MS. 2019. Interferon lambda protects the female reproductive tract against Zika virus infection. *Nat Commun* 10:280. <https://doi.org/10.1038/s41467-018-07993-2>
94. Casazza RL, Philip DT, Lazear HM. 2022. Interferon lambda signals in maternal tissues to exert protective and pathogenic effects in a gestational stage-dependent manner. *mBio* 13:e0385721. <https://doi.org/10.1128/mbio.03857-21>
95. Kang S, Narazaki M, Metwally H, Kishimoto T. 2020. Correction: historical overview of the interleukin-6 family cytokine. *J Exp Med* 217. <https://doi.org/10.1084/jem.2019034704212020c>
96. Clark AR, Dean JLE. 2016. The control of inflammation via the phosphorylation and dephosphorylation of tristetraprolin: a tale of two phosphatases. *Biochem Soc Trans* 44:1321–1337. <https://doi.org/10.1042/BST20160166>
97. Zhang X, Chen X, Liu Q, Zhang S, Hu W. 2017. Translation repression via modulation of the cytoplasmic poly(a)-binding protein in the inflammatory response. *Elife* 6:e27786. <https://doi.org/10.7554/eLife.27786>
98. Bayer A, Lennemann NJ, Ouyang Y, Bramley JC, Morosky S, Marques ETDA Jr, Cherry S, Sadovsky Y, Coyne CB. 2016. Type III interferons produced by human placental trophoblasts confer protection against Zika virus infection. *Cell Host Microbe* 19:705–712. <https://doi.org/10.1016/j.chom.2016.03.008>
99. Shalem O, Sanjana NE, Hartenian E, Shi X, Scott DA, Mikkelsen T, Heckl D, Ebert BL, Root DE, Dönnch JG, Zhang F. 2014. Genome-scale CRISPR-Cas9 knockout screening in human cells. *Science* 343:84–87. <https://doi.org/10.1126/science.1247005>
100. Sanjana NE, Shalem O, Zhang F. 2014. Improved vectors and genome-wide libraries for CRISPR screening. *Nat Methods* 11:783–784. <https://doi.org/10.1038/nmeth.3047>
101. Nabbi A, Riabowol K. 2015. Rapid isolation of nuclei from cells *in vitro*. *Cold Spring Harb Protoc* 2015:769–772. <https://doi.org/10.1101/pdb.prot083733>